University of California, San Diego
Institute of Pure and Applied Physical Sciences
La Jolla, CA 92093

Final Technical Report

"Pure Electron Plasmas Near Thermal Equilibrium"

1 Jun 82 — 30 Sep 90

Supported by

Office of Naval Research

ONR N00014-82-K-0621

Principal Investigators:

Prof. J. H. Malmberg
Dr. C. F. Driscoll
Prof. T. M. O'Neil

Other Scientific Staff:

Dr. F. Anderegg
Prof. D. H. E. Dubin
Dr. K. S. Fine
Dr. A. W. Hyatt
Mr. T. Mitchell
Prof. M. Rosenbluth
Dr. R. A. Smith

Visitor:

Prof. Roy Gould

November 1990

Statement "A" per telecon Dr. Charles Roberson. Office of Naval Research/code 1112AI.

VHG 1/8/91

INTRODUCTION

Since 1982 the plasma group at UCSD has been conducting an experimental and theoretical program of research on Pure Electron Plasmas Near Thermal Equilibrium, supported by the Office of Naval Research under contract ONR N00014-82K-0621. This document gives an overview of the scientific results from this program, and lists the technical publications which are the most complete description of these results. The experiments were carried out on a pure electron plasma containment apparatus built under sponsorship of ONR; the theory research was in support of these experiments and other related topics. By any scientific measure, both the experiments and the theory program were very productive. These programs are presently continuing and expanding under sponsorship of ONR, with a new laser-diagnosed ion apparatus under construction which will enable stimulating new experiments.

Plasmas are the central element in many physical systems, including devices to generate radiation or high intensity beams of particles. Plasma effects are important in modern high current accelerator concepts, especially collective effect accelerators. They are central to the thermonuclear reactor problem, and of course outdoor plasmas dominate the physics of a large portion of the known universe. The physics of these systems can be very complex, and most of the devious ways by which plasmas manage to cross magnetic fields are not yet well understood.

At UCSD we have sought to obtain tests of plasma theory under the simplest possible circumstances we can devise; and, when the theory is inadequate, to develop it further. The ultimate motivation of the work has been to improve our understanding for application to a variety of physical systems. The direction for the program has been determined by the apparatus and by the internal logic of the science which we are attempting to expand.

The present program has been an outstanding success, both experimentally and theoretically. Under ONR sponsorship we built a device designed to contain a pure electron plasma in thermal equilibrium and to observe the transport processes that take the plasma to thermal equilibrium. The effort succeeded and the thermal equilibrium has been observed. We originally expected that the traditional theory of particle transport due to collisions would be essentially correct in describing the evolution to equilibrium. However, in the course of predicting the operation of the new machine, we realized that the traditional transport theory was implicitly based on a particular ordering of plasma parameters which did not apply to magnetically confined single-species plasmas. We needed to develop a whole new transport theory for this case. A

substantial portion of this new theory has been completed. It predicts that the rate of transport to thermal equilibrium is much faster and the physics is very different. This greatly enhanced transport is observed experimentally.

Recently we have been experimentally investigating the transport associated with fluid instabilities, which is much faster than collisional transport. In this work we investigate the dynamics of hollow density profiles which have a substantial shear in their drift rotation profiles. These hollow profiles exhibit an initial diocotron mode shear instability, which is the plasma analogue of the Kelvin-Helmholtz fluid instability. The instability undergoes nonlinear saturation with the formation of vortices, then the vortices decay into turbulent noise, and finally the noise decays leaving a reasonably quiet quasi-equilibrium. The collisional transport to thermal equilibrium then occurs on a much longer time scale. We have also observed an unusual $l = 1$ instability which the previously published theoretical literature stated unconditionally was stable. The vortex merging phase is, in one limit, mathematically identical to the physics of two-dimensional inviscid fluids and we have pursued this scientific connection.

The machine has also proved to be of great value for other experiments we did not initially envision. One of these has provided a high precision test of the rate at which an asymptotic temperature distribution relaxes. A second involves greatly enhanced internal transport by what we believe is a two-wave plus resonant particle collective effect. A third experiment has elucidated the nonlinear properties of the off-axis dynamical equilibrium of the system which is frequently referred to as the $l = 1$ diocotron mode. Experiments on plasmas near the Brillouin limit have contributed to our understanding and increased our confidence in the predicted operation of the new ion apparatus.

We have also developed a scaling theorem which states that under certain conditions the orbits of each particle in an ion machine will be identical to the orbit of a corresponding electron in an electron machine. The conditions are that the magnetic field is increased by the square root of the mass ratio, the sign of applied voltages is reversed, corresponding ions and electrons have the same energy, radiation is unimportant, and only classical effects determine the motion. This scaling theorem has enabled design of the ion containment apparatus.

Another important theoretical effort supported by the program is a combined simulation and analytic study of clusters. Here, a comparatively small number of confined ions are so cold that they are strongly coupled in the sense that Γ, the ratio of

the interaction potential energy to the kinetic energy, is large. This theory is more directly applicable to the elegant trap experiments at Boulder than to the current UCSD work. The calculations show that as Γ is increased, first a liquid-like order is observed and then ordering in nested shells where their axes are aligned parallel to the applied magnetic field. This ordering is similar to that of a smectic liquid crystal. At larger values of Γ a distorted 2-D hexagonal lattice within a given shell will occur beginning with the outermost shell. This intricate series of ordering processes which is due to the finite size of the system is much richer than the simple plasma to liquid to solid transitions expected for an infinite system. This work has recently been extended to consider the vibrational normal modes of these clusters. Close and productive cooperation between the theorists at UCSD and the experimentalists at Boulder exists.

A totally unexpected area of theory research developed on the properties of "negative temperature," off-axis equilibria of 2D plasmas or vortices. These equilibria result from maximizing the Vlasov entropy subject to required conservation laws. In certain parameter regimes, it is most probable to find the plasma displaced off the axis of the containment system. However, the relation between these 2D thermal equilibria and the off-axis diocotron modes observed experimentally is not yet clear.

These research areas are described in somewhat more detail in the next section. However, for technical details the reader is referred to the published works referenced here.

RESEARCH RESULTS

The Electron Containment Apparatus (EV)

This research program began with the design and construction of a new experimental apparatus. The design was based on an extrapolation from previous devices, and this extrapolation proved to be valid: the measured plasma lo[illegible] times at low magnetic fields and base pressures are substantially longer than the theoretically predicted times for approach to thermal equilibrium. We have thus been able to quantitatively study the transport towards equilibrium, under conditions where the external couplings causing plasma expansion and loss are small perturbations. The apparatus has the capability of making density and temperature measurements as a function of radius and time, so we are able to completely determine the fluid characteristics of the plasma.

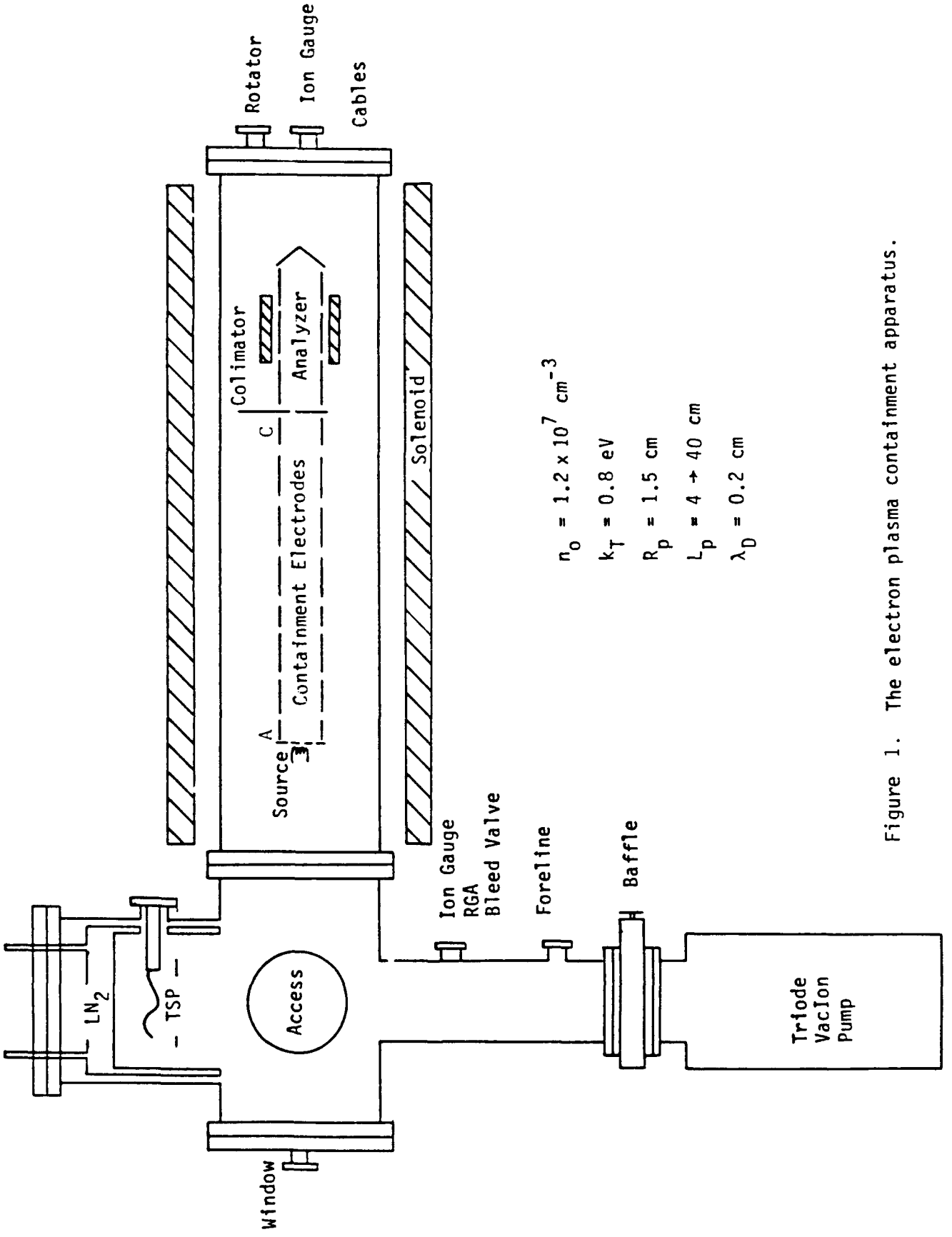

Figure 1. The electron plasma containment apparatus.

A schematic of the EV apparatus is shown in Figure 1. The apparatus consists of a filament source, cylindrical containment electrodes, and a velocity analyzer and collector. These are enclosed in an ultra-high-vacuum chamber in a uniform axial magnetic field. During both design and construction, prime consideration was given to minimizing cylindrically asymmetric couplings to the plasma. The acronym EV derives from Equilibrium plasma, Voltage containment.

Radial confinement of the plasma is provided by a uniform static axial magnetic field B. The end electrodes are biased sufficiently negatively that axial confinement of the electron plasma is assured. The plasma column is rotating, since the radial electric field due to space charge gives an $\mathbf{E}\times\mathbf{B}$ drift in the $\hat{\theta}$ direction. The electron plasmas contain a negligible number of positive ions, since ions are not confined longitudinally. The magnetized column of electron gas is a plasma by the criterion that the Debye length is small compared to the radius of the column.

The trapped electrons may be transported across the field by various processes. A variable time (t) after injection, the electrons are dumped out the end. The machine includes collectors behind collimating holes in the end plate of the machine, so the density at a particular radius and angle, $n(r,\theta,t)$, may be measured. We also analyze the electrons as they are dumped to obtain the temperatures $T_{\parallel}(r)$ and $T_{\perp}(r)$ characterizing the plasma. $T_{\parallel}$ is obtained by measuring the number of electrons which are energetic enough to escape axially as the containment voltage V_c is slowly made less negative. We obtain $T_{\perp}$ by use of a "beach analyzer" utilizing a secondary magnetic field. Essentially, this method uses an electrostatic velocity analyzer to measure the change in the parallel energy of exiting electrons caused by the secondary field. Techniques for longitudinal compression and "stacking" of nonneutral plasmas have been extensively developed. The plasma density and radius can also be modified by magnetic field "ramping" -- i.e., increasing or decreasing the magnetic field after the plasma has been captured.

With the current containment electrodes, typical values of the injected electron density and thermal energy are $n=10^7$ cm^{-3} and $kT=0.8$ eV, although these may be varied by more than an order of magnitude. The nominal plasma and wall radii are $R_p=1.5$ cm and $R_w=3.8$ cm, while the plasma length can be varied over the range $L=4-40$ cm. For our typical parameters, the Debye length $\lambda_D=(kT/4\pi e^2 n)^{1/2}$ can be computed to be $\lambda_D\approx 0.2$ cm; the electrons thus constitute a plasma by the criterion that $R_p \gg \lambda_D$.

Our first experiments[2] on the EV apparatus established that the plasma confinement times are substantially larger than those obtained from the previous device. This improvement derives from a decrease in the neutral gas pressure, and from a reduction of construction asymmetries in the magnetic and electric fields. The dominant losses on EV and on the previous device are due to small construction asymmetries. These asymmetries in the magnetic or electric field structures cause losses which depend strongly on the length L of the plasma column, as well as on the magnetic field B. The new EV apparatus was constructed with particular attention given to minimization of these asymmetries, in order to obtain the longer confinement times required to observe transport to equilibrium. The magnetic solenoid was wound more accurately, the use of permeable materials was minimized, and the cylindrical containment electrodes were fabricated and aligned to closer tolerance.

The measured confinement times τ_m on EV scale as $(L/B)^{-2}$ over a range of 5 decades.[2] Interestingly, this is the same scaling with L/B as was observed on the previous apparatus. However, the EV confinement times are on average a factor of 20 times longer than those from the prior apparatus. The EV data includes plasma lengths from 4 to 40 cm, and magnetic fields from 33 to 375 Gauss. The EV confinement scaling is

$$\tau_m = (32 \text{ sec}) \left[\frac{L}{10 \text{ cm}}\right]^{-2} \left[\frac{B}{100 \text{ Gauss}}\right]^{2} .$$

This confinement scaling suggests the dominance of a single transport mechanism in both apparatuses, although this process has not yet been identified. Since all containment devices have asymmetries, we believe this transport will be generic to all non-neutral plasma experiments in this geometry.

Given enough time, the electrostatic interactions between electrons will bring the plasma to thermal equilibrium. These interactions conserve angular momentum and cannot lead to a loss of electrons; so the thermal equilibrium state must correspond to a confined set of electrons. The one-electron thermal distribution (Boltzmann distribution) is given by

$$f = n_0 \left[\frac{m}{2\pi kT}\right]^{3/2} \exp\left[\frac{-1}{kT}(H - \omega p_\theta)\right] ,$$

where $H = \frac{1}{2} m v^2 - e\phi(r,z)$ is the Hamiltonian for an electron and $p_\theta = m v_\theta r - (eB/2c) r^2$ is the canonical angular momentum for an electron. The

parameters n_0, T, and ω are determined by the number of electrons, the energy, and the angular momentum in the system. This distribution may be rewritten in the form

$$f = n(r,z)\left[\frac{m}{2\pi kT}\right]^{3/2} \exp\left[\frac{-m}{2kT}(\mathrm{v}-\omega r\hat{\theta})^2\right] \quad ,$$

where

$$n(r,z) = n_0 \exp\left[\frac{e\phi(r,z)}{kT} - \frac{m}{2kT}(\Omega\omega-\omega^2)r^2\right]$$

and $\Omega = eB/mc$.

The density is essentially constant out to a certain radius R_p, then falls exponentially toward zero in a few Debye lengths. The velocity distribution is a Maxwellian at temperature T when viewed in a frame rotating with angular velocity ω. One can think of the possible equilibrium profiles as being parametrized by the central density n_0, the plasma radius R_p, and the temperature T.

Transport to Equilibrium: Experiments

Construction of the EV apparatus with long containment times has enabled the first observations of transport to global thermal equilibrium.[3,5,6,10] The plasma evolves to a state in which the temperature is radially uniform and the density profile is such as to give rigid drift rotation, as expected. However, the time required for transport to equilibrium differs significantly from the predictions of traditional like-particle transport theory: the equilibration times are orders of magnitude smaller, and scale approximately as B^1 or B^2 instead of as B^4. The first equilibration times obtained from EV scaled roughly as B^2, whereas a more rigorous data set obtained later scaled accurately as B^1. These two data sets were obtained from substantially different initial plasmas, and it is now predicted theoretically that the dominant transport mechanism depends on the plasma density profile.

From the fluid perspective, the evolution to equilibrium is determined by the time evolution of the plasma density $n(r,z,t)$ and (isotropic) temperature $T(r,t)$. An example[10] of the experimentally measured evolution towards global thermal equilibrium is shown in Figure 2. Here, we show the density profiles $n(r,z=0)$ and rotation profiles $\omega(r) = \mathrm{v}_\theta(r,z=0)/r$ at three different times. Initially, the density is low in the center and peaked at the edge. This profile evolves monotonically towards a shape of the thermal equilibrium form. Of course, the true test of the density profile

being appropriate for equilibrium is whether the rotation profile is uniform. As shown in Figure 2, the initially injected plasma has substantial shear, rotating about 40% faster on the edge than in the center. As particles and heat are transported radially, the rotation profile evolves to essentially rigid rotation. The temperature profile also becomes uniform during this evolution.

To obtain a characteristic time τ_{eq} for the particle transport towards equilibrium, we calculate how "far" the density profile at any given time is from the final equilibrium profile. This "distance" $D(t)$ is essentially the radial integral of the difference between the two profiles. We find that $D(t)$ decreases as $e^{-t/\tau_{eq}}$ as the plasma relaxes toward equilibrium, and τ_{eq} is unambiguously determined. Using this method, we have obtained characteristic times τ_{eq} over a range of fields B from 47 to 470 G, as shown by the solid triangles in Fig. 3. We find that τ_{eq} scales closely as B^1, implying transport rates scaling as B^{-1}. For this series, we tried to keep the initial plasmas as alike as possible as B was varied. All profiles had a non-monotonic $n(r)$ and $\omega(r)$.

We had previously measured the equilibration times for substantially different plasma profiles at slightly higher densities, using much less rigorous techniques. These rough estimates for τ_{eq} are shown as open circles with factor-of-two error bars, scaling approximately as B^2. The two data sets differ most at low magnetic fields where these rough estimates are generally least reliable.

The experimental scaling of $\tau_{eq} \alpha B^1$ for plasmas with non-monotonic $n(r)$ (and consequently non-monotonic $\omega_E(r)$) stimulated theory development for this case. It now appears that a new non-local "resonant rotation" transport mechanism may be important when $\omega_E(r_1) = \omega_E(r_2)$ for some r_1 and r_2 in the plasma. Theory predicts that transport times from this process alone should scale as B^1. The transport rates are difficult to compute for realistic plasmas, but estimates are consistent with the experimental data. In contrast, when $\omega_E(r)$ is monotonic, theory predicts that only the local "collisional $\mathbf{E} \times \mathbf{B}$ drift" transport should appear. Transport times would then scale approximately as B^2.

The experiments clearly show that a new type of transport much stronger than traditional Boltzmann transport is operating in our plasmas; but the experiments do not yet verify any particular theory. The possibility of two new transport processes makes the experiments more interesting, but makes the experimental analysis more difficult. We are presently pursuing these measurements, and incisive tests of the various theories appear probable.

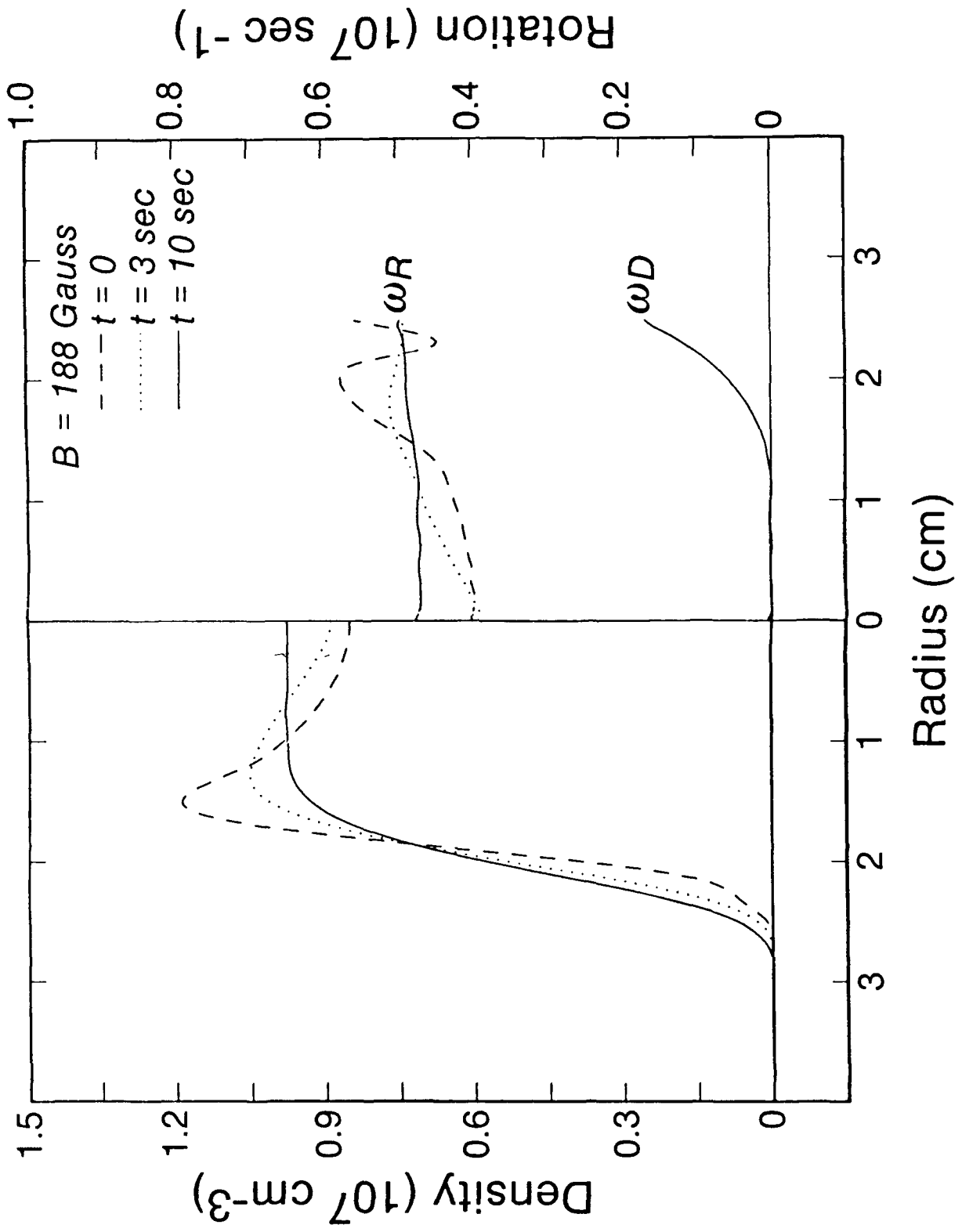

Figure 2. Experimental plasma density profiles n(r,t) and rotation profiles $\omega_R(r,t)$ at three different times t, showing the evolution to equilibrium. Also shown is the diamagnetic drift $\omega_D(r)$ at t = 10 sec.

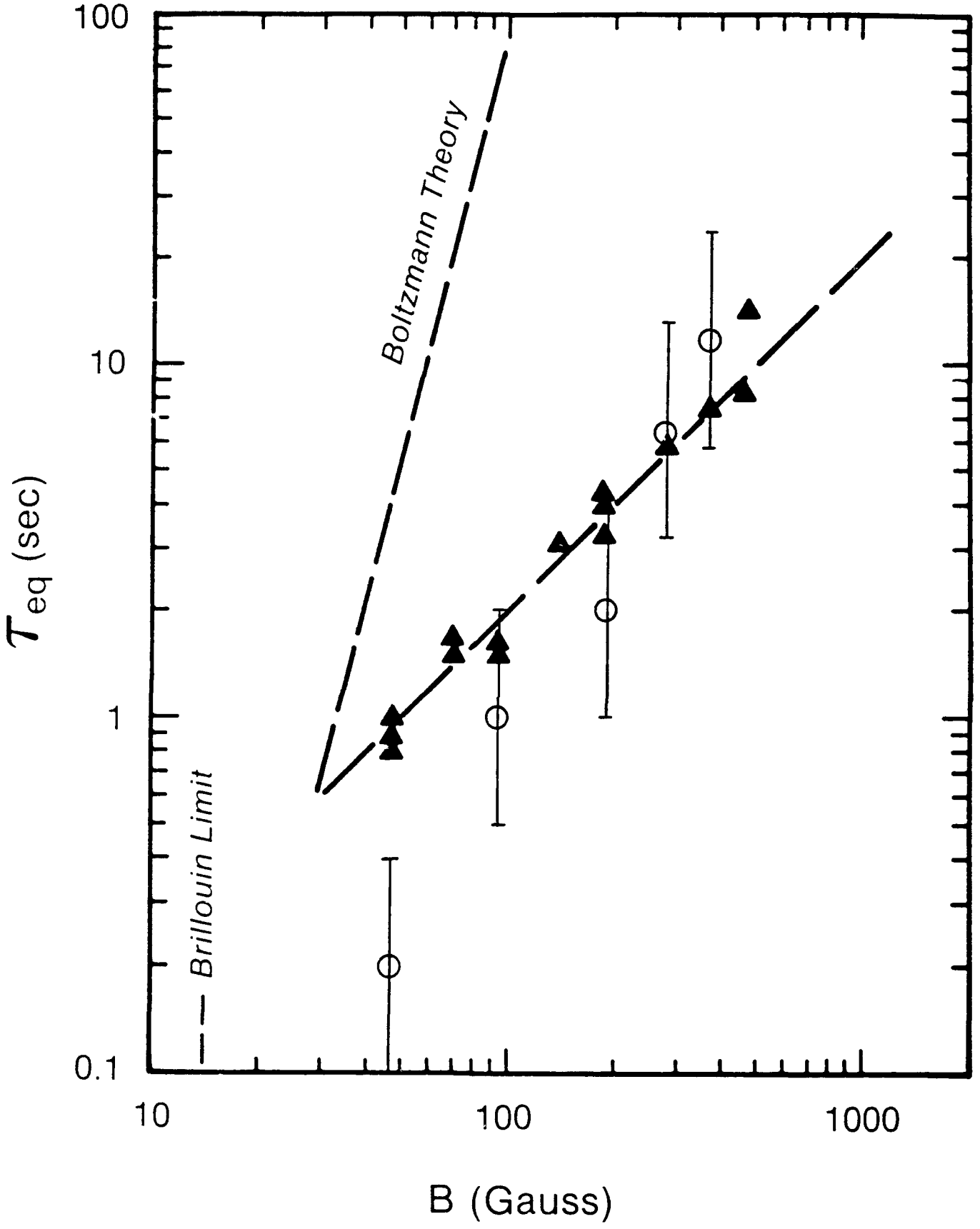

Figure 3. Experimentally measured relaxation times τ_{eq} (triangles) versus magnetic field B for non-monotonic plasma densities.[4] The lower dashed line is $\tau_{eq} \propto B^1$; the upper dashed line is an estimate from traditional transport theory. Also shown as circles with factor-of-two error bars are the original experimental estimates of τ_{eq}.

Transport to Equilibrium: Theory

The problem of transport due to like-particle collisions is an old and venerable problem in plasma theory. It was considered in the early years of the CTR program by Simon and by Longmire and Rosenbluth. These authors had in mind ion-ion collisions in a neutral plasma, and for this case the Larmor radius of the colliding particles typically is much larger than the Debye length ($r_L \gg \lambda_D$). We now know from theoretical arguments and from experimental measurements that this traditional theory does not provide an adequate description of like-particle transport in the regime where $r_L \ll \lambda_D$, and this is the operating regime for magnetically confined nonneutral plasmas.

While performing theoretical studies in support of the transport experiments, we discovered a new transport mechanism which is neglected in the traditional theory.[1,3,5,6,11] The basic idea is that two electrons which are too far apart to undergo collisional velocity scattering (the mechanism invoked in the traditional theory) can still undergo collisional $\mathbf{E}\times\mathbf{B}$ drifts, where $\mathbf{E}$ is the interaction electric field. Such collisions are neglected in the traditional theory, and as a result our new theory predicts a much larger flux than the traditional theory.

Furthermore, the scaling of the magnitude of the particle flux with magnetic field strength differs. In the traditional theory, flux scales as B^{-4}. However, in the new theory the $\mathbf{E}\times\mathbf{B}$ drift interactions break naturally into two classes, one of which leads to particle flux whose magnitude scales as B^{-2}, the other producing flux scaling as B^{-1}. In the former class electron pairs are assumed to collide only once as they stream past one another on adjacent field lines separated by distances on the order of λ_D. In the latter case electrons interact many times as they bounce back and forth between the ends of the plasma column.

The distinction between the two types of $\mathbf{E}\times\mathbf{B}$ collision can be understood if we note that the interation field produced by electron 2 is effective in producing transport of electron 1 only if electrons 1 and 2 interact resonantly. They must satisfy a resonance condition of the form $kv_1 + l\omega_E(r_1) = kv_2 + l\omega_E(r_2)$, where v_1 and v_2 are the velocities of electrons 1 and 2 along the magnetic field, and $\omega_E(r_1)$ and $\omega_E(r_2)$ are the $\mathbf{E}\times\mathbf{B}$ rotation frequencies. The interaction is effected through a Fourier component characterized by axial wave number k and azimuthal mode number l.

For large values of k such that $k\mathbf{v} \gg \omega_E$ (where $\mathbf{v}$ is the thermal speed), the resonance condition reduces to $kv_1 = kv_2$; these Fourier components lead to B^{-2} scaling. For small k, the condition reduces to $l\omega_E(r_1) = l\omega_E(r_2)$; in this case B^{-1}

scaling is obtained. Furthermore, this latter resonance condition can be satisfied for $r_1 \neq r_2$ only if the rotation frequency $\omega_E(r)$ is nonmonotonic in r. Since r_1 and r_2 can be separated by distances on the order of the plasma radius, the interactions are long range; the particle flux at any given position therefore depends on the global state of the plasma.

From a fluid perspective, the radial electric field (space charge field) and radial pressure gradient produce an azimuthal fluid drift

$$v_\theta(r) = -\frac{c}{B}\left[E_r + \frac{T}{en}\frac{\partial n}{\partial r}\right] \quad .$$

In general, this fluid velocity has shear, and the shear produces a viscous force in the azimuthal direction. In turn, this azimuthal force produces a radial drift, and this drift is the particle flux

$$\Gamma_r = \frac{c}{eB}\frac{1}{r^2}\frac{\partial}{\partial r}\left[r^2 \eta r \frac{\partial}{\partial r}\left[\frac{v_\theta(r)}{r}\right]\right] \quad ,$$

where η is the coefficient of viscosity.

In general, the coefficient of viscosity is of the form

$$\eta = nm\, \nu\, (\Delta x)^2$$

where ν is the electron-electron collision frequency and Δx is a length scale characteristic of the collisional dynamics. The new theory and the traditional theory yield different predictions for Δx, namely, $\Delta x \cong \lambda_D$ and $\Delta x \cong r_L$, respectively. Thus, the ratio of the flux predicted by the new theory to the flux predicted by the traditional theory is $(\lambda_D / r_L)^2 \gg 1$. Consequently, the new theory and the traditional theory yield different predictions for the scaling of the flux with magnetic field strength, namely, $\Gamma_r \propto B^{-2}$ and $\Gamma_r \propto B^{-4}$, respectively.

In summary, all of the previous theory (traditional theory) was based on a solution of the Boltzmann equation (or Lenard-Balescu equation) for an inhomogeneous plasma. This equation includes the effect of velocity scattering (through the collision operator) but not of collisional **E**×**B** drifts. To include this effect, one must start further back in the analysis, that is, with the Klimontovitch equation. Since the collisions which make the dominant contribution to the viscosity may be described by guiding center theory, we have based our new analysis on a guiding center model of the equation.

We obtain an expression for the flux which is of the same form as that given in Eq. (8), and the coefficient of viscosity is given by

$$\eta_{new} = \frac{\sqrt{\pi}\sqrt{m}\, e^4 n^2}{6(kT)^{3/2}} \ln\left(\frac{\nu}{\Delta\nu}\right) - \nu mn\lambda_D^2 \quad .$$

Here, the logarithmic term relates to a cut-off in the velocity integral, and $\Delta\nu/\nu$ is the larger of $(\nu/\omega_p)^{1/3}$ or r_L/λ_D. The ratio of this coefficient of viscosity to that used in the traditional theory is

$$\frac{\eta_{new}}{\eta_{trad.}} = \frac{5}{12}\left[\frac{\ln(\nu/\Delta\nu)}{\ln(r_L/b)}\right]\left[\frac{\lambda_D}{r_L}\right]^2 \quad ,$$

where $b = e^2/kT$ is the classical distance of closest approach.

Anisotropic Temperature Relaxation

Another experimental program on EV addressed the local velocity-space equilibration which occurs on each field line.[8,29] In these experiments, we change the parallel temperature $T_\parallel$ by axial compression or expansion, and then measure the time evolution of $T_\parallel$ and $T_\perp$ as they relax to a common value. This yields a relaxation rate which can be obtained as a function of density and temperature, providing a quantitative verification of a sophisticated statistical theory.

A theoretical description of collisional velocity scattering has been the subject of continuing effort over the past 50 years. Small momentum transfer collisions are thought to dominate, which has led to a Fokker-Planck approximation to the velocity scattering process. Many important theoretical results have been obtained with this approach. However, there have been only a few direct experimental tests of the theory, and these tests have uncertainties of order unity.

Ichimaru and Rosenbluth (IR) calculate the rate of anisotropic temperature relaxation in a weakly magnetized one-component plasma for which the Larmor radius r_L is much larger than the Debye shielding length γ_D, i.e. $r_L \gg \gamma_D$. They employ the "dominant term" approximation, which neglects all terms that do not contain the Coulomb logarithm, $\ln\Lambda$, factor in the rate. Since terms of relative order $1/\ln\Lambda$ are neglected, the theoretical rate is calculated only to that accuracy, which in our plasma is about 10%.

We can adapt the small magnetic field calculation of IR to our experimental regime of $r_L \gg \lambda_D$ by using a general result of Montgomery, Joyce and Turner. MJT

have shown that, to good approximation, zero and small magnetic field transport theories can be applied in the $r_L < \lambda_D$ regime if the argument of the Coulomb logarithm is changed from $\Lambda = \lambda_D / b$ to $\lambda = r_L / b$, where $b = e^2/T$ is the classical distance of closest approach. This change can be thought of as a decrease in the range over which effective collisions can occur. The effect of the MJT approximation in our experimental regime is to reduce the theoretical rate of IR by approximately 25%.

When we compare our experimental results with the predictions of this theory we find agreement to within approximately 10% over a two decade range, as shown in Fig. 4. This is an absolute comparison, since there are no adjustable parameters in either the theory or the experimental measurements. In this data, we vary the density between 3×10^6 and 3×10^7 cm^{-3}, and vary the temperature between 0.7 and 8 eV, while the magnetic field is held constant at 280 Gauss. The line is the absolute prediction of collisional relaxation, modified to cut off Coulomb logarithm at r_L instead of λ_D.

This experiment formed the basis for the Ph.D. thesis of Dr. Alan Hyatt.[29]

Fluid Instabilities and Turbulence

The plasma columns which have been observed to evolve to thermal equilibrium have been axially short ($L_p \sim 3\, R_p$), and have therefore been stable with respect to shear-driven fluid instabilities. However, if similar non-monotonic density profiles are created in long plasma columns ($L_p \sim 20\, R_p$), Kelvin-Helmholtz instabilities with large growth rates are observed.[14,15,18,22,24] These instabilities result in large-scale cross-field transport on a time scale of 100 μsec, that is, about 10^4 times faster than the "collisional" transport described in the previous section. This transport proceeds until the plasma is no longer unstable, by virtue of having an essentially monotonically decreasing density profile.

We studied unstable systems for a number of reasons. First, these fluid instabilities occur in many plasma and hollow beam systems, but have not been quantitatively studied. We can study the dynamical evolution accurately (with no averaging) from controlled initial conditions with varying degrees of instability. Since we obtain an accurate map of $n(r,\theta,t)$, we can calculate the potential $\phi(r,\theta,t)$. Thus the 2-D drift dynamics of the plasma is completely determined, to the extent that it can be considered an infinite length system.

An example of this instability-driven evolution is shown in Figure 5, which displays the density $n(r,\theta)$ in false color at four different times. Here, an initial

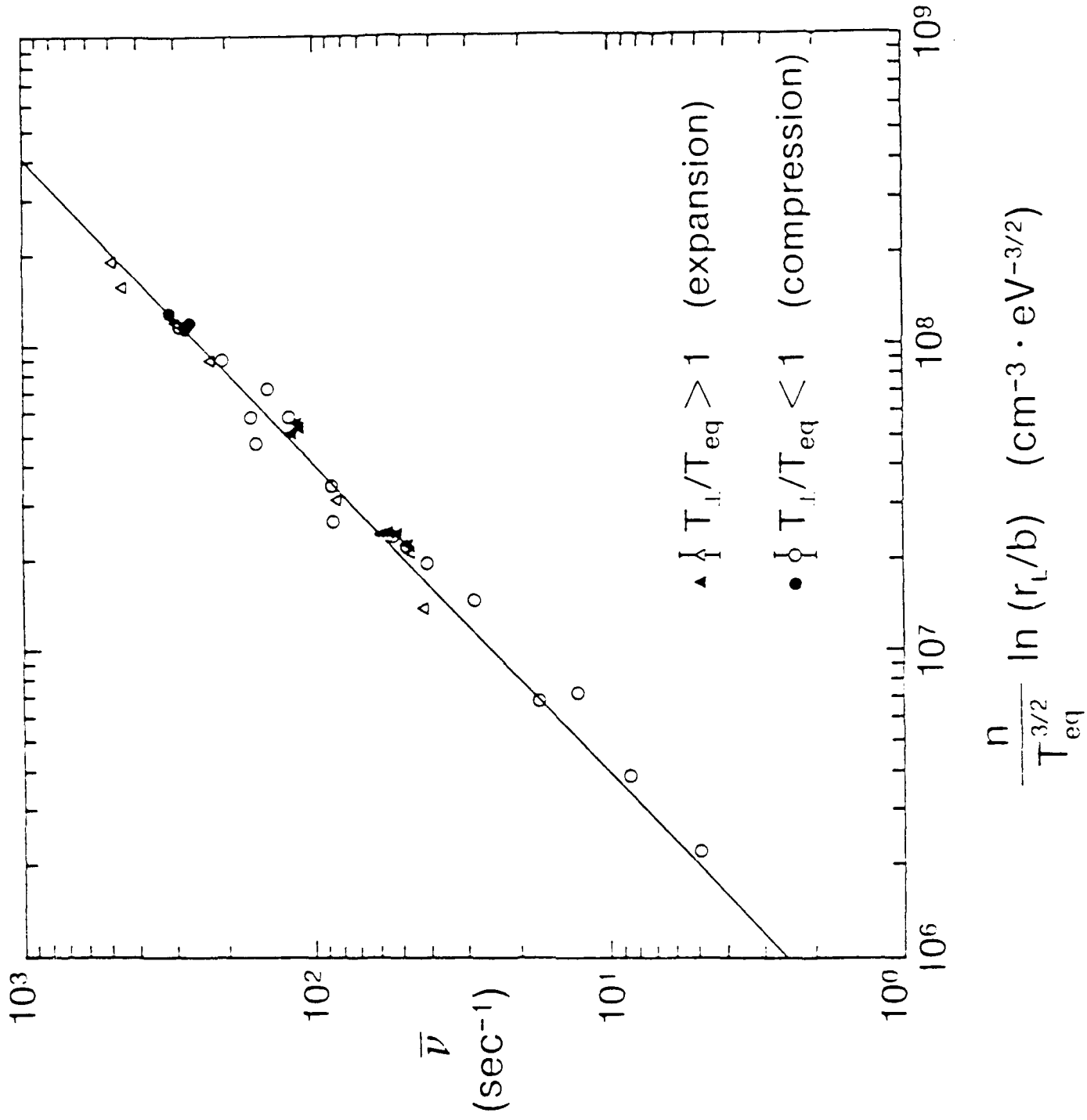

Figure 4. Experimentally measured relaxation rates $\bar{\nu}$ for various electron plasma densities and temperatures. The solid line is the absolute prediction of theory.

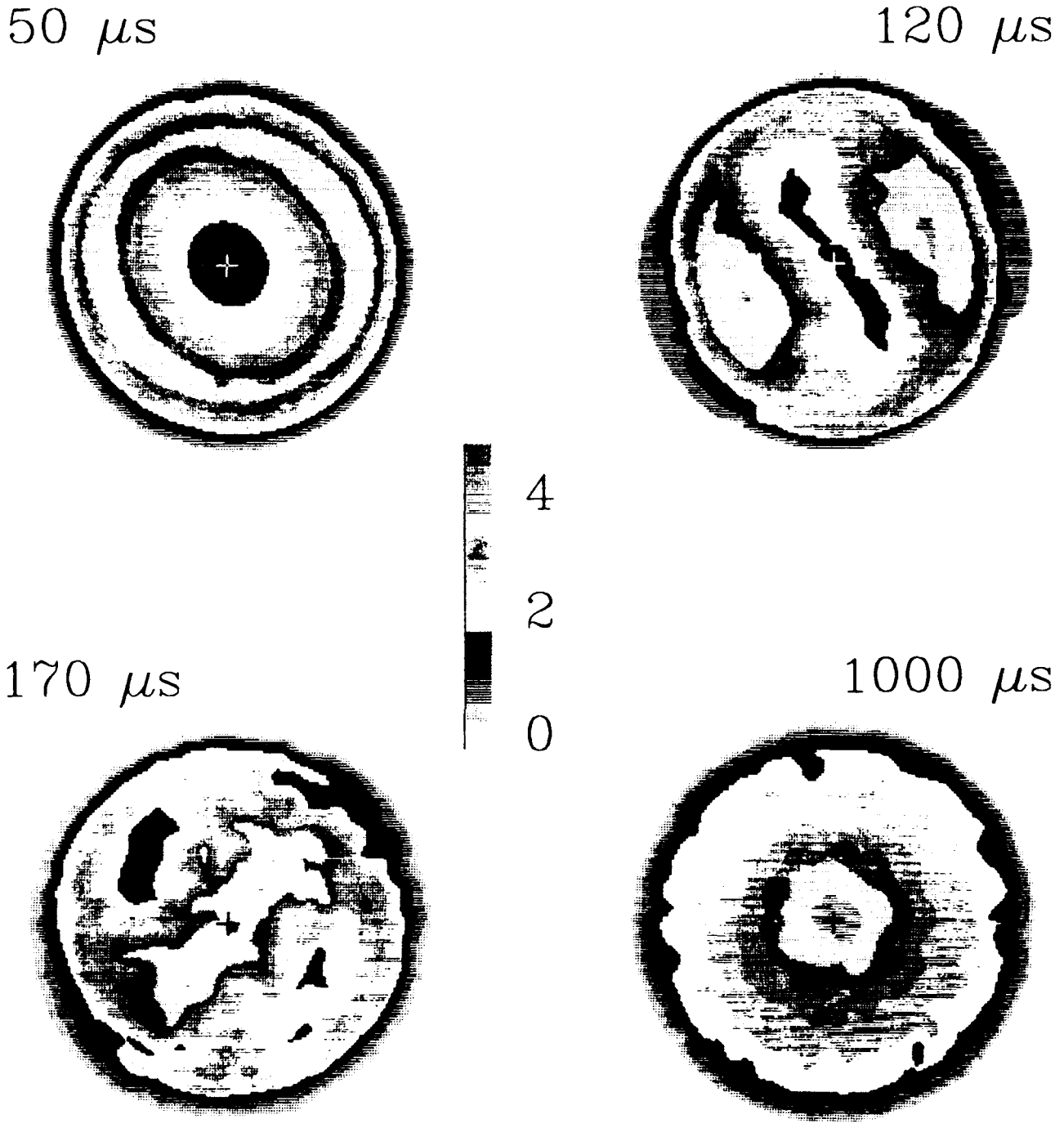

Figure 5. False-color density plots showing n(r,θ) at 4 different times as an $\ell=2$ instability grows on a hollowed profile (a) forming vortices (b) which merge and disintegrate (c) to give a stable monotonically decreasing profile (d).

plasma column is made hollow by ejecting some of the electrons near $r=0$. This gives a plasma which has a central density about 50% of the edge density, giving an $\mathbf{E}\times\mathbf{B}$ drift profile with strong rotational shears. This plasma is quite symmetric in the θ direction, except for a very small deliberately launched seed wave with azimuthal mode number $l=2$ (*i.e.* varying as $\sin(2\theta)$). This seed wave grows exponentially on a time scale of 30 μsec, until it saturates with the formation of two nonlinear vortex structures. These vortices rotate about each other and about their own centers, until they merge and form chaotic density variations on smaller spatial scales. The resulting 20% noise fluctuations decay on a time scale of several hundred microseconds, leaving a monotonically decreasing plasma density.

For $l=2$, this exponentially unstable mode is observed for a wide range of hollow profiles,[14,15,22] and these results are basically consistent with 2D theory predictions. These modes vary as $\delta n(r)\exp\{ikz+il\theta-i\omega t\}$, with $k=0$ for the 2D modes considered here. Numerical solution of the eigenvalue equation for realistic smooth profiles has given fair agreement with unstable $l=2$ growth rates in these preliminary experiments.

When we seed the hollow profile with an $l=1$ perturbation, we observe a similar instability, as shown in Figure 6. We are able to observe exponential mode growth over a range of up to 2 decades before nonlinear saturation occurs.[18,22] The instability appears to be a linear process, i.e. independent of the perturbation amplitude at $t=0$. Typically, the instability e-folds in about 6 rotation periods for the column. The measured amplitude of the unstable mode is shown in Figure 7.

In contrast, prior theory had concluded that there are no instabilities for $l=1$. More recent theory work has elucidated an instability which grows algebraically with time, but this is not a full explanation.[19] The theoretical growth with time can be obtained by numerically integrating a linear Laplace transform solution which starts from initial conditions corresponding to the experiments. Alternately, one can perform an asymptotic analysis on the Laplace transform solution, obtaining a perturbation proportional to $t^{1/2}$ as $t\to\infty$. The theoretically predicted mode growth is shown by the dashed line in Figure 7.

Although the differences between experiment and theory here are large, there are intriguing similarities. The early time instability growth is seen to be similar. Further, the time-asymptotic theory perturbation is self-shielding,[6] as is observed experimentally at all times.[5]

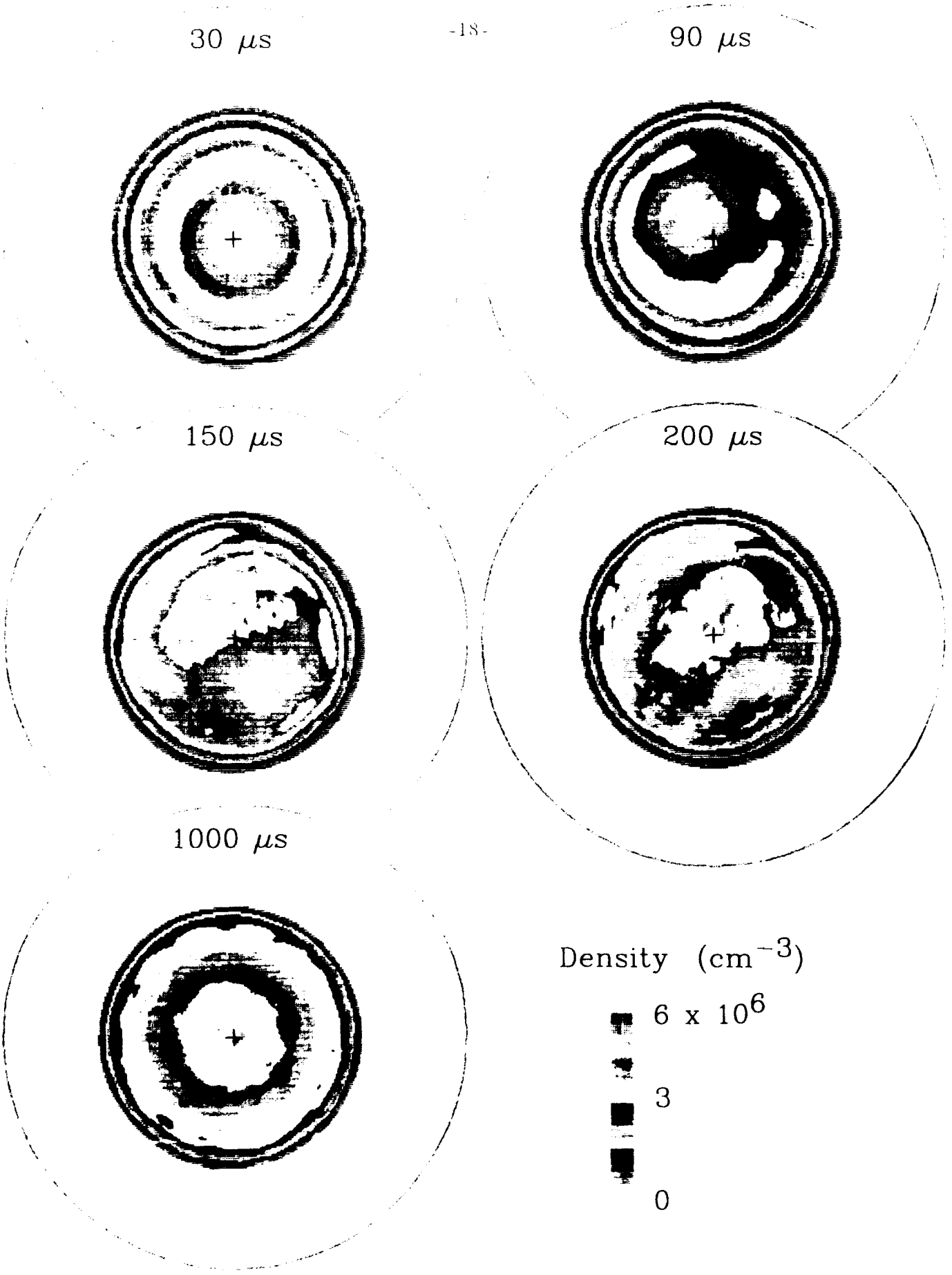

Fig 6 Measured density $n(r,\theta)$ at 5 times in the evolution of a hollow column which had a small $l = 1$ perturbation at $t = 0$.

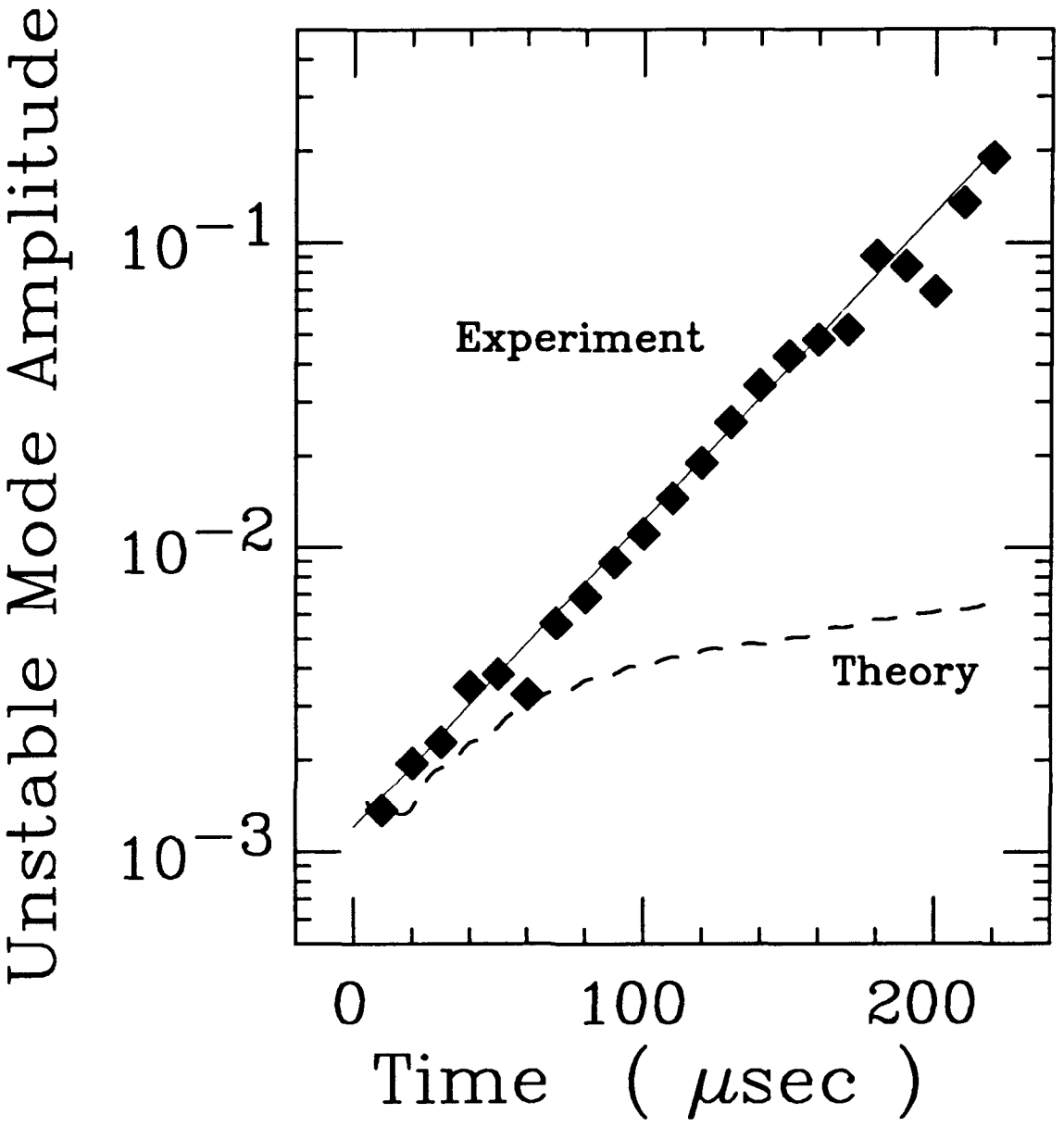

Figure 7. Experimentally measured unstable $\ell = 1$ mode amplitude (diamonds) versus time. Also shown is the algebraically growing perturbation predicted by theory.

In addition to providing the initial rapid phase in the evolution of an unstable column to thermal equilibrium, the instabilities are of interest in their own right. In the plasma context, there is a substantial literature and a long history concerning these instabilities; they have been studied for about 40 years. Also, it turns out that the full nonlinear equations used to describe these modes (Poisson's equation plus 2-D $\mathbf{E}\times\mathbf{B}$ drift dynamics) are isomorphic to the equations used to describe shear instabilities (Kelvin-Helmholtz) in the inviscid shear flow of an ordinary fluid; the plasma density corresponds to the vorticity and the electric potential to the stream function.[22] In this sense, one may think of the pure electron column as an ideal low viscosity fluid that models some classic problems in 2-D fluid dynamics.

In our theoretical studies of these instabilities we were joined by Roy Gould, who was on sabbatical at UCSD during the 88-89 academic year. We developed a shooting code and a relaxation code to determine the eigenmodes, growth rates and frequencies for arbitrary density profiles, and we compared these results to those for special profiles (e.g., stair case profiles) that can be treated analytically. Our goal was to develop a general intuitive understanding of the instability criterion and of the number of modes for an arbitrary density profile.

We developed a 2-D particle in cell simulation in which the particles (long rods parallel to the field) move according to $\mathbf{E}\times\mathbf{B}$ drift dynamics. The Poisson solver is consistent with cylindrical geometry, and we use the boundary condition $\phi(r=R_w,\theta)=$constant, where R_w is the radius of a cylindrical conducting wall. The code is vectorized to run efficiently and time for runs was provided by a grant from the San Diego Supercomputer Center. Runs of reasonable duration (1 hour of Cray time) follow the dynamics through the growth of the instabilities and well into the stage of nonlinear relaxation.

Vortex Dynamics

The two vortex merger process can be studied as an isolated process, independent of any diocotron instability process. In a sense, this is a generalization of our recent work on the (stable) nonlinear $l = 1$ diocotron mode,[20,22,30] which may be thought of as a single vortex interacting with a wall. Straightforward manipulation techniques allow us to form an initial condition consisting of two electron columns of chosen profile and placement. Here, we consider the particular case of two equal columns which are placed symmetrically on either side of the cylindrical axis, separated by a distance 2D.

We observe that the behavior of the two vortices depends dramatically on their separation to diameter ratio. If the vortices are separated by more than 1.7 diameters, we observe that they orbit around each other relatively unperturbed for up to 10^4 orbits. If the vortices are initially separated by 1.5 diameters, their mutual interaction quickly results in filamentary tail formation, but the vortices still orbit around each other for about 100 orbits before merging at the center. If they are separated by 1.4 diameters, we observe merger at the center in less than one orbit period, as shown in Figure 8.

A plot of the time requred to merge versus the initial vortex separation is shown in Figure 9. The merger time abruptly increases from 10 μsec to about 1 sec as the separation varies from 1.4 to 1.7 diameters. The upper limit of 1 second represents about 10^5 orbits, and probably reflects unwanted experimental couplings. Nevertheless, the data clearly establishes the critical distance for merger.

We have varied the vortex radius R_p by a factor of two, and find that the merger time does indeed scale as the ratio of the vortex separation to the vortex diameter. For our analysis, the diameter is defined by $2R_p \equiv 3\int dA\ nr'/\int dAn$, where r' is relative to the center-of-mass. This suggests that this is a reasonable definition of diameter for density profiles with a smooth edge, although there are other definitions that give similar results (and others that give less satisfactory results). Furthermore, the wall radius does not enter the scaling, indicating that the mutual interaction of the vortices dominates over wall interactions.

This may represent the cleanest experimental measurement to date of this fundamental vortex interaction process. The low inherent viscosity of the plasma and the total absence of boundary layers at the wall both contribute to absence of secondary effects which could obscure its result. These preliminary results are in agreement with theory and computational results, and with a much more qualitative experiment in a water tank at Australian National University.

The orbit frequency and vortex shape distortion can also be measured as a function of separation of the two vortices. We find that the orbit frequency is well-modelled by the interaction of 2 "point" vortices of appropriate total circulation (*i.e.* total charge per unit length axially), but that the wall interaction must be included for large separations. We also find that the interacting vortices elongate towards each other even in the absence of merger. The elongation appears roughly consistent with various "moment models" and numerical calculations, but the experimental data has not yet been analyzed in detail.

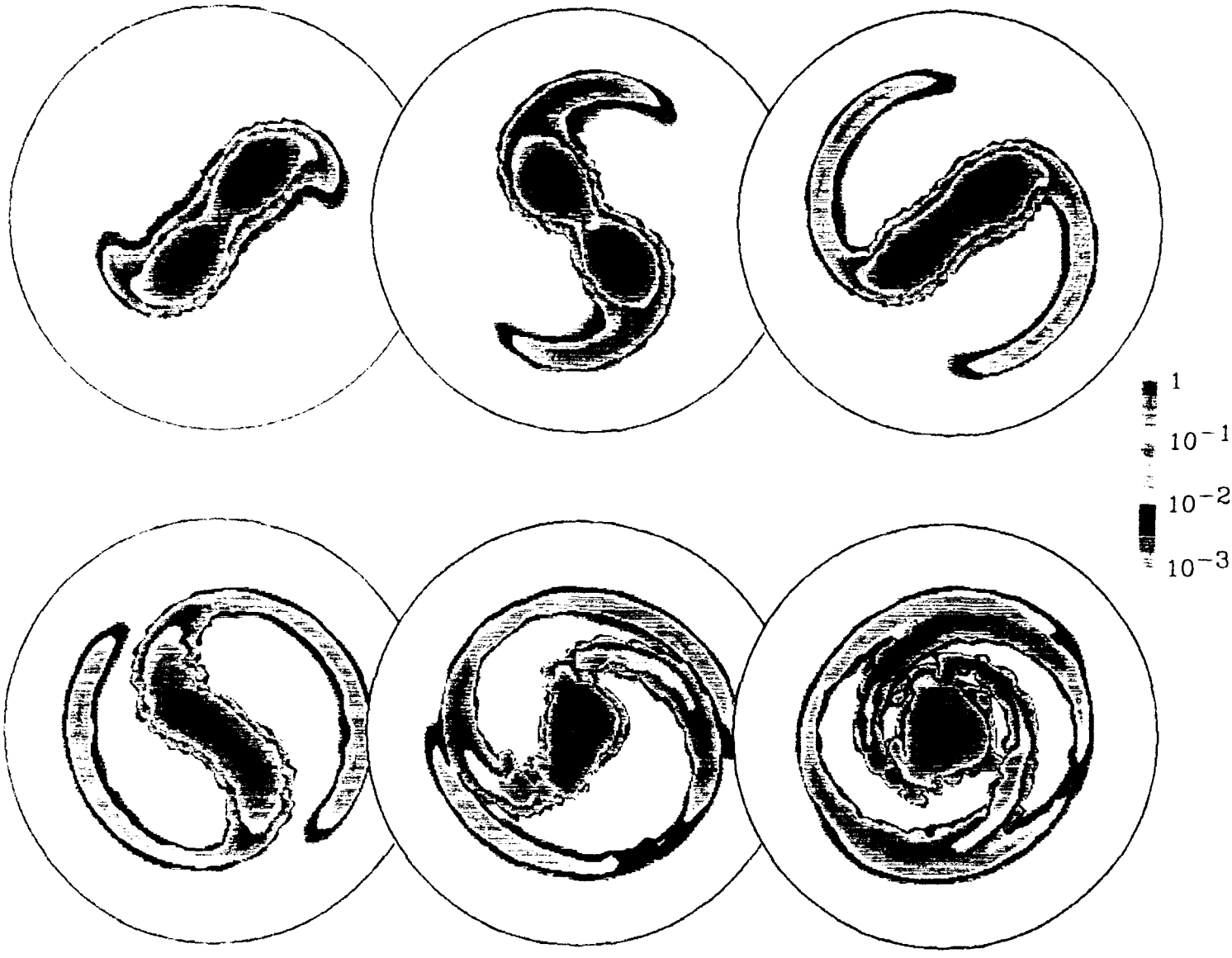

Fig 8 Measured density $n(r,\theta)$ at 6 times during the merger of 2 vortices initially separated by 1.4 vortex diameters. Time intervals are 10 μsec.

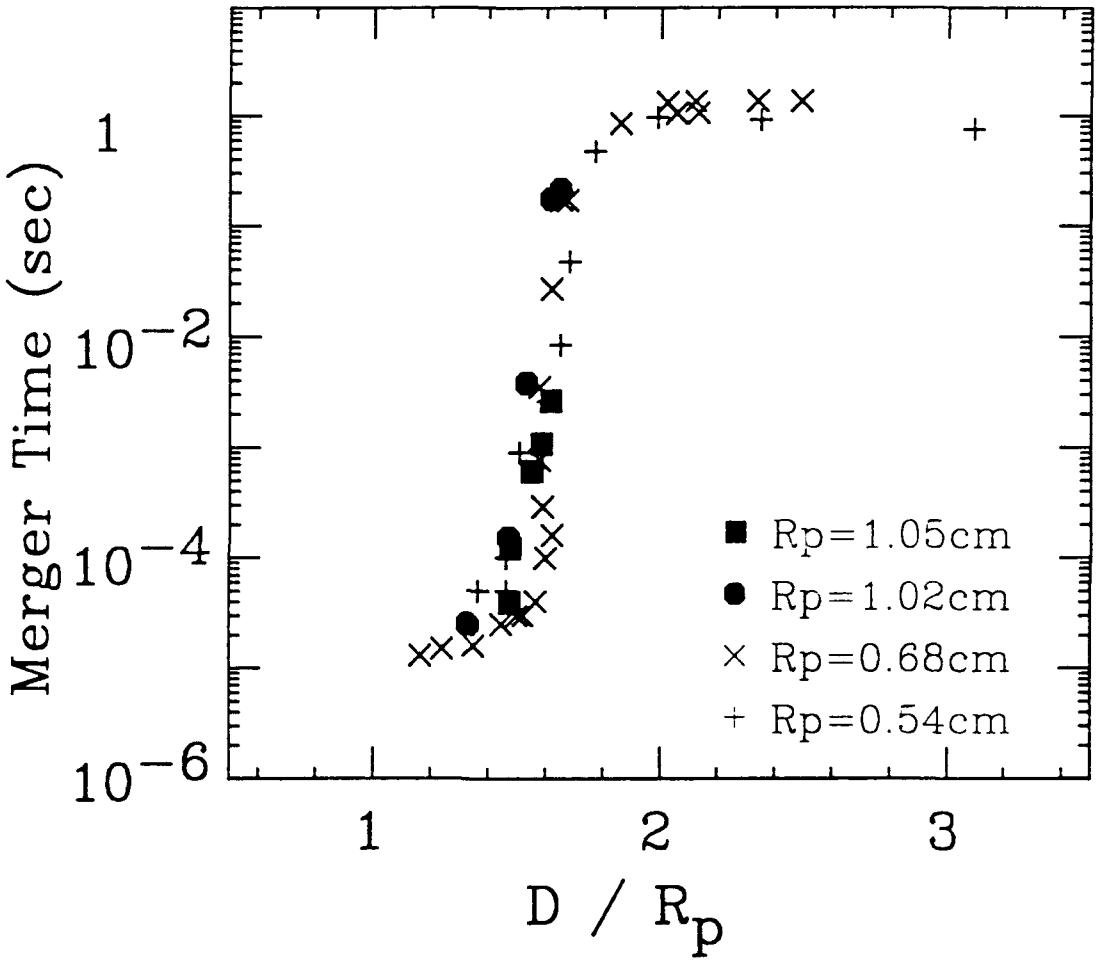

Figure 9. Experimentally measured merger time versus the ratio of vortex separation 2D to vortex diameter $2R_p$, for vortices of various diameters.

Negative Temperature Equilibria

Theoretically, one candidate for the configuration resulting from vortex mergers or violent shear-flow instabilities is the "most probable state" obtained by maximizing the Vlasov entropy $S = -\int n \ln n$ of the distribution of guiding centers, subject to the constraints imposed by certain conservation laws. In the continuum limit, the integral of any function of density is conserved. Nonideal dissipation or coarse-graining eliminates the small scales of turbulence, and breaks the conservation of all but the simplest of these functionals. Hence only a few gross conservation laws may survive.

We have analytically studied the equilibria which result from taking the total charge, the canonical angular momentum, and the electrostatic energy to be the only conserved quantities.[17,21,28] (This assumes that the guiding-center degrees of freedom are decoupled from velocity space over the time scales which characterize turbulent relaxation.) The constrained maximum-entropy configurations are then guiding-center thermal equilibria, described by the equation

$$n(r,\theta) = n_0 \exp\{-\beta(e\phi - \omega r^2)\} \quad ,$$

where the parameters n_0, β, and ω are determined by the charge, energy, and angular momentum.

We find that "negative temperature" solutions exist for certain parameter regimes and that these equilibria are displaced from the geometrical center of the system at large energies or angular momenta. Such an off-axis state can be regarded as a dynamic equilibrium or equivalently as a finite-amplitude diocotron mode. $1/\beta$ is an effective temperature, and is negative for the off-axis equilibria. These results have been confirmed by Monte Carlo simulations of ensembles of guiding centers. We find that the statistical fluctuations can be surprisingly large, much as in a system undergoing a phase transition. However the relation between these thermal equilibria and the final states or stable diocotron modes observed in experiments is not yet clear.

Strongly Correlated States and Normal Modes

When a single species plasma in thermal equilibrium is cooled to a sufficiently low temperature, it passes first into the liquid state and then into a crystalline state. The theory of these states is well understood for infinite sized systems with no boundaries: this system is called the One Component Plasma (OCP). Computer simulations and analytic theory for an infinite homogeneous OCP predict that for $\Gamma \geq 2$ the system of charges begins to exhibit local order characteristic of a liquid, and for

$\Gamma \geq 172$ there is a first-order phase transition to a bcc crystal.

However, the physics is substantially more complicated for clusters of $10^2 - 10^4$ particles. In our cryogenic electron plasma experiments, $\Gamma \sim 1-2$ have been achieved; in ion plasma experiments at NIST, Γ values in the range of several hundred have been measured, putting the system well into the regime of strong correlation.

We have studied the properties of these finite-sized clusters using a combination of analytic theory and computer simulation.[9,16,23,25,26] For moderate values of Γ ($2 < \Gamma \leq 100$) we find that the density of the cloud exhibits spatial oscillations. These oscillations have maximum amplitude at the cloud surface and decay back to the background density n_0 with increasing distance from the surface. The oscillations are evidence of local order, and the damping length is a measure of the correlation length. For $\Gamma \geq 140$, the cloud separates into concentric spheroidal shells. In this regime charges rarely move from shell to shell, but they diffuse freely within the shell surfaces. Thus, the system might be characterized as a liquid within the shells, and as a solid in the direction perpendicular to the shells, as in a smectic liquid crystal. For still larger values of Γ particle diffusion within the shells also approaches zero and an imperfect 2-D hexagonal crystal is formed within each shell.[9] An example of such a structure is shown in Figure 10.

We find that the lattice structure in the crystalline regime is quite different from the bcc lattice predicted for an infinite homogeneous OCP. Simulations have been performed on up to 2000 ions, and no evidence of bcc structure has been observed. Recent theoretical work based on the extremely oblate "slab" limit of the bounded crystal predicts that the system may have to be quite large before the minimum energy state displays bcc symmetry, perhaps requiring as many as 60 shells before the infinite homogeneous structure is recovered.[16] Thus, the addition of a surface term to the free energy can change the thermal equilibrium lattice structure, even if this surface term is relatively small compared to the bulk term.

In order to extend this result to finite temperatures, the internal energy of the classical one component plasma was calculated analytically in the crystalline phase for both fcc and bcc lattices to $O(T^2)$ (that is, to the lowest order in which anharmonic phonon-phonon interactions contribute to the energy).[23] This calculation uncovered a conceptual error in all previous calculations for the past 20 years: This $O(T^2)$ term was previously assumed to be negligible, yet we find it to be rather large, contributing at least half of the internal energy due to anharmonic interactions. This increases the thermodynamic stability of the crystal phase over previous estimates, shifting the phase

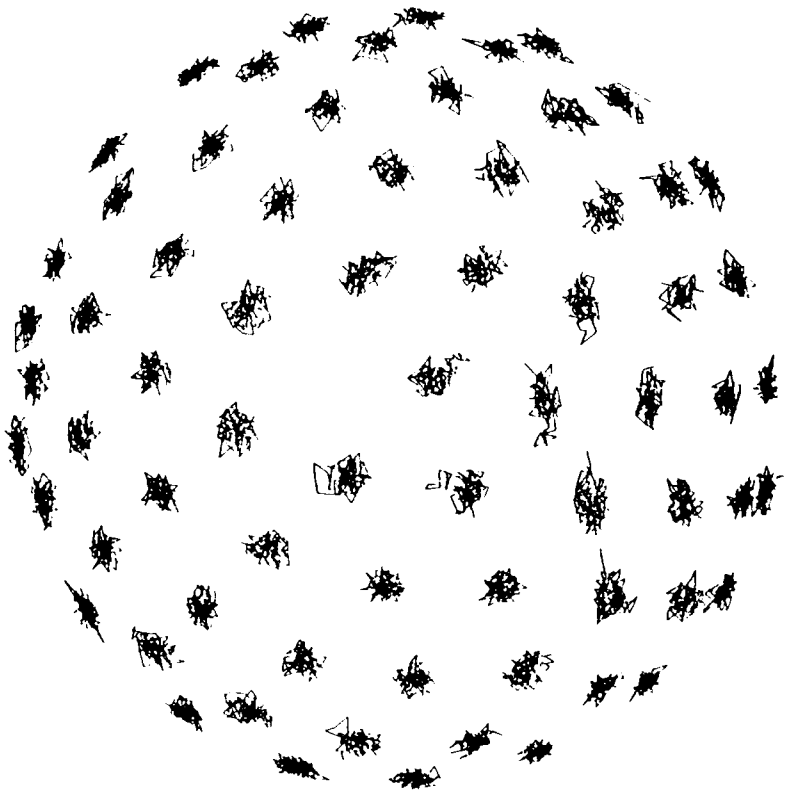

Figure 10A. Projection of ion orbits from half of outer shell onto x-y plane in the rotating frame, showing distorted 2-D hexagonal lattice. N = 256, Γ = 380, ω_z/Ω_c = 0.1.

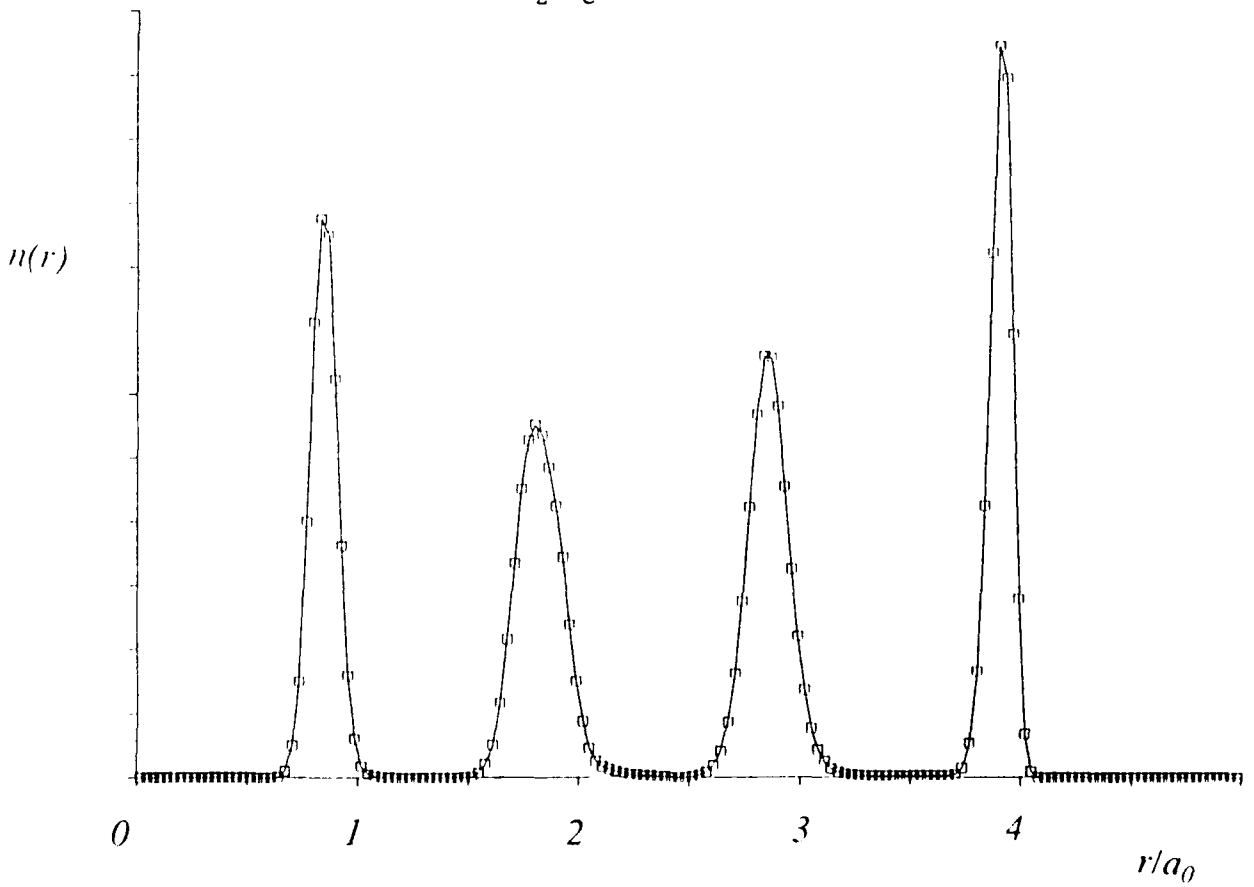

Figure 10B. Time-averaged density versus radius.

transition to $\Gamma \sim 172$ from its previous value of $\Gamma \sim 180$.

Recently, we have considered[26] the fluid normal modes of oscillation of the ion clouds confined at NIST. These normal modes can be excited by either sinusoidally oscillating the electrode potentials at a mode frequency, or by the introduction of a static field error which can resonate with a zero-frequency mode. Due to the spheroidal shape of the cloud and the presence of the strong magnetic field, the wave equation for the modes does not appear to be separable at first glance. However, we have obtained a separable solution to the eigenmode problem which describes the fluid modes in a cloud of any spheroidal shape. The effect of correlations and viscosity on these modes is presently being considered.

Ion-Electron Scaling

Much of the physics of nonneutral plasmas applies equally to both ion and electron plasmas, with a simple scaling between the two.[4] The Newton-Maxwell equations for particles of mass m and charge Ze are

$$\frac{d^2\mathbf{r}_j}{d\tau^2} = e\left[\boldsymbol{\varepsilon}(\mathbf{r}_j) + \frac{1}{c}\frac{d\mathbf{r}_j}{d\tau}\times\mathbf{b}(\mathbf{r}_j)\right] ,$$

$$\nabla\cdot\boldsymbol{\varepsilon} = 4\pi e\sum_j \delta(\mathbf{r}-\mathbf{r}_j) \quad , \quad \nabla\cdot\mathbf{b} = 0$$

$$\nabla\times\boldsymbol{\varepsilon} = -\frac{1}{c}\frac{\partial\mathbf{b}}{\partial\tau} \quad , \quad \nabla\times\mathbf{b} = \frac{Z^2}{m}\left[\frac{4\pi e}{c}\sum_j \frac{d\mathbf{r}_j}{d\tau}\delta(\mathbf{r}-\mathbf{r}_j) + \frac{1}{c}\frac{\partial\boldsymbol{\varepsilon}}{\partial\tau}\right] ,$$

where

$$\tau = |Z|m^{-1/2}t ,$$

$$\boldsymbol{\varepsilon} = Z^{-1}\mathbf{E} ,$$

$$\mathbf{b} = m^{-1/2}\frac{Z}{|Z|}\mathbf{B} .$$

The equation of motion and the first three of Maxwell's equations are completely scaled with respect to charge and mass. In the electrostatic approximation, the ion and electron cases are identical provided that the magnetic field is reversed in direction and scaled by the square root of a mass ratio, and that the electric field is scaled by Z. The scaling requires the initial kinetic energies differ by Z^2, vis.

$$\frac{1}{2}\left|\frac{d\mathbf{r}_j}{d\tau}\right|^2 = \frac{1}{Z^2}\frac{m}{2}\left|\frac{d\mathbf{r}_j}{dt}\right|^2 .$$

Of course, the ion case runs slower by a factor $(m_i/m_e Z^2)^{1/2}$. Only the $\nabla \times \mathbf{b}$ equation does not scale. Thus, for those ion plasma effects that are electrostatic in nature, an electron plasma experiment will give analogous results.

However, the electron and ion systems are not completely identical. Corrections to $\mathbf{b}$ due to particle and displacement currents will be smaller by $(m_e Z^2/m_i)$ for the ion plasma. Cyclotron radiation, which gives an energy loss rate $\dot{W} = 2q^2\dot{v}^2/3c^3$, is proportional to $(Ze)^4 B^2 m^{-3}$, at a given energy. Thus, radiation can be an important cooling mechanism for electrons, but not for ions because it is slower by a ratio $(m_i/m_e)^3$. We note, however, that cyclotron radiation is not important on the EV electron apparatus, so the electron and ion plasmas would be analogous in this parameter regime. The physics associated with two or more species of all ions all with the same sign of charge but with different values of $|z/m|$ is also not reproduced by the electron system. The most important difference between electron and ion plasmas, however, results from the fact that the collision of an ion with another object must be described with quantum mechanics. Such collisional effects are not subject to the above scaling.

These scaling laws were the basis for design of the new pure ion plasma apparatus (IV) which is being built under support from ONR.

Plasmas Near the Brillouin Limit

For a single unneutralized charge species, the maximum density which can be contained in a given magnetic field is set by the Brillouin limit, $\omega_p^2 \le \Omega_c^2/2$; or equivalently, $nmc^2 \le \frac{B^2}{8\pi}$. The Brillouin limit is a statement that the $\mathbf{v} \times \mathbf{B}$ force must balance the electrostatic force due to space charge and the centrifugal force. (Here we ignore kT, which is normally much smaller.)

We have studied the physics of plasmas near the Brillouin limit as the next step in extending our experiments into parameter regimes of practical applicability, as for high brightness sources of electrons or positrons for various experiments, including radiation producing devices. Ion containment devices in general operate close to the Brillouin limit, since the attainable magnetical fields are limited.

For our usual electron operating parameters, the density n is far below that corresponding to the Brillouin limit, n_B, and the orbits of the electrons are small diameter cyclotron orbits slowly drifting around the axis of the machine. The orbit frequency in the rotating frame is given by the so-called vortex frequency,

$\omega_v = \omega_c - 2\omega_r$ where ω_c is the cyclotron frequency and ω_r is the rotation frequency of the plasma. As the Brillouin limit is approached, the radius of the orbits becomes large, the rotation frequency becomes $\omega_c/2$ and the vortex frequency approaches zero.

The angular momentum constraint becomes substantially less simple as one approaches the Brillouin limit. As the density gets near the Brillouin limit, the mechanical part of the angular momentum becomes comparable to the vector potential part and both terms must be kept. At the Brillouin limit the two terms are equal in magnitude and the angular momentum is zero.

The experimental procedure for investigating plasmas with density near the Brillouin limit is straightforward. We simply inject a long, moderate density plasma into the machine, allow it to evolve into a quiescent state, and then compress it longitudinally with symmetric electrostatic potentials applied by containment cylinders. Since this increases the density without increasing the magnetic field and without adding any angular momentum to the system, the plasma will necessarily approach the Brillouin limit.

Our initial guess was that if the compression was sufficient so that a pure longitudinal compression would produce an n greater than n_B, then the plasma would just expand radially somewhat. The expansion would keep the density below the Brillouin limit, leaving the plasma stably contained. However, this is not always what happens. In experiments utilizing axial compression to create temperature anisotropy, we often find that as we got within a factor of about 10 of the Brillouin limit, the loss rate increased rapidly; and as we compressed more, the plasma disappeared abruptly from the machine.

Several new and interesting transport processes may contribute to this process. Asymmetry-induced transport increases near the Brillouin limit, so new resonances not involving the longitudinal bounce motion are possible when $n\omega_v - m\omega_r = 0$. These resonances may produce strong resonant particle transport as soon as the vortex frequency ω_v begins to approach the rotation frequency ω_r. This presumably would look experimentally like a rapid diffusive process. Another possible process is that the plasma is being driven unstable by a wave process or multi-wave process.

Our recent experiments in this regime on EV have suggested that a wave instability occurs substantially after the density compression occurs. This instability may be associated with field asymmetries, since it appears similar to instabilities observed on the V' apparatus when asymmetries were introduced. Since EV has smaller asymmetries, the instability is not observed at all in normal operation, but is

apparently enhanced as the Brillouin limit is approached.

Induced Wave Damping and Transport

In another series of experiments on the EV apparatus, we have studied transport resulting from the interaction between waves and the particles.[30] A great deal of plasma transport theory is concerned with the resonant wave-particle interaction, and we are studying one of the simplest such cases associated with the $l=1$ diocotron wave. Here, the wave varies as $\exp\{il\theta+ikz-i\omega t\}$. This diocotron wave is a dynamical equilibrium in which an off-center plasma column drifts around the axis of the containment cylinders.[20] Normally, no electrons are resonant with this mode, and damping is small. Experimentally, we observe essentially no change in the wave amplitude over a time of several seconds (*i.e.* $\sim 10^5$ cycles).

If we apply a static perturbation voltage to one of the containment cylinders, the wave is observed to damp.[30] As a result of the damping, the off-center column becomes a centered column of larger diameter, as shown in Figure 11. The radial profiles are obtained by dumping the plasma synchronous with the wave phase, essentially a stroboscopic density measurement. This data shows that the plasma has indeed broadened as the wave damps, corresponding to radial transport. This transport does not carry the plasma to the wall, but rather leads to internal rearrangement. This radial transport conserves angular momentum as expected for an axisymmetric external perturbation.

We interpret this process as two waves interacting nonlinearly to produce a beat wave which is resonant with some plasma particles. In our case, one wave is the $l=1$, $k=0$ diocotron mode; and the second wave is the perturbation field, with $l=0$, $k\neq 0$, $\omega=0$, which is not a normal mode of the plasma. This interaction has been elucidated by the induced scattering theory of Crawford and O'Neil. One prediction of the nonlinear theory is that the damping is exponential and scales as the perturbation voltage squared. This signature is observed in some parameter regimes. We feel this may be one of the simplest, most understandable examples of induced transport.

Nonlinear and Finite Length Diocotron Modes

Measurements have been made of the frequency and phase-locked density $n(r,\theta)$ of a large amplitude diocotron mode.[20,30] The diocotron mode is essentially an offset of the plasma column from the conducting wall axis by a displacement, D. The electric field can be calculated using the method of images: the image charges in the

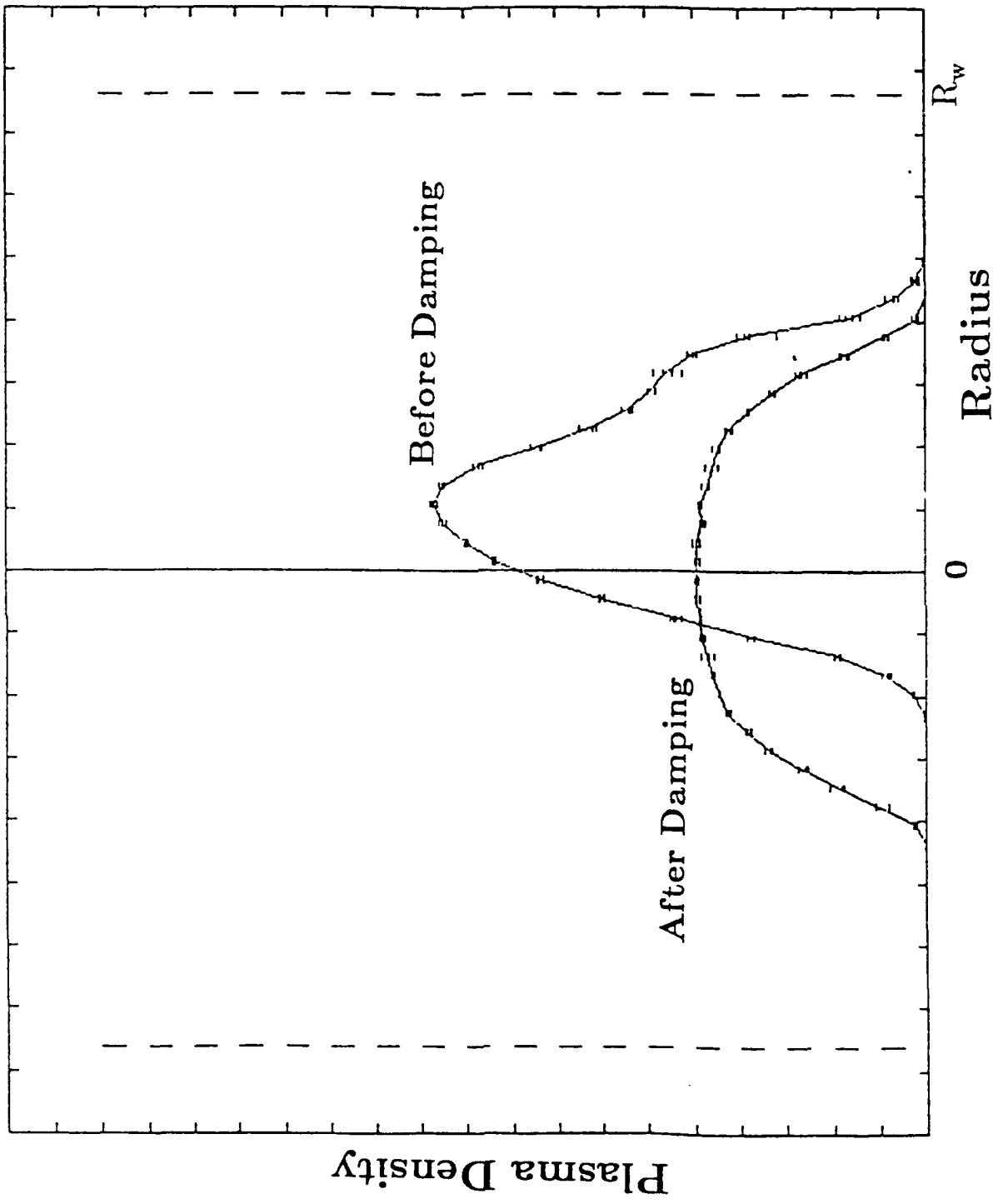

Figure 11. Stroboscopic cross-section of the plasma density n(r) before and after a large amplitude $\ell = 1$ diocotron wave is damped by a $\ell = 0$ perturbation.

conducting wall are replaced by a rod of charge at a particular position outside the wall. The diocotron motion is the $\mathbf{E}\times\mathbf{B}$ drift of the column in the electric field of this image charge. We find that prior theories are inadequate at describing the mode at large amplitude, but that most effects can be understood from the image charge model.

The mode frequency shifts from its low amplitude value by an amount proportional to D^2. This frequency shift is understood as being due to two effects: 1) the plasma is closer to its image charge than a linear model assumes, and 2) the plasma distorts from a circular shape. From the plots of $n(r,\theta)$, it can be seen that at large amplitudes the column shape becomes elliptical with elongation in the θ-direction. The distortion and frequency shifts are in excellent agreement with a theoretical waterbag model. The model is based on the assumption that the plasma density is time invariant in a frame rotating at the diocotron frequency, as is observed experimentally.

Finite length effects are important even for small amplitude diocotron modes. We have measured the diocotron frequency as a function of L_p and plasma radius, R_p. The image charge model predicts a mode frequency, f_d, that depends only upon charge per unit length in the column. We have found that the measured frequency, f, is up to 200% higher in short plasmas. The fractional frequency shift $(f-f_d)/f_d$ increases as L_p^{-1} and decreases with R_p. This is in reasonable agreement with a finite length theory of Prasad and O'Neil.

Finite length theory suggests that couplings to other plasma modes may induce damping in the $l=1$ diocotron mode. We have measured the damping rate of the finite length diocotron mode at various B_z and amplitudes. In all cases, the diocotron mode was found to not be damped to within the accuracy of the measurement. The quality factor, Q, of this resonance was determined to be greater than 10^7. The measurements indicate that the mode damping is at least three to four orders of magnitude smaller than the theory predicts. The discrepancy is not understood at this time.

This research, together with the experiments on induced wave damping and transport, formed the basis for the Ph.D. thesis of Dr. Kevin S. Fine.

PUBLICATIONS LIST, ONR N00014-82-K-0621

Journal Articles

1. T. M. O'Neil, "New Theory of Transport Due to Like-Particle Collisions," *Phys. Rev. Lett.* **55**, 943 (1985).
2. C. F. Driscoll, K. S. Fine and J. H. Malmberg, "Reduction of Radial Losses in a Pure Electron Plasma," *Phys. Fluids* **29**, 2015 (1986).
3. C. F. Driscoll and T. M. O'Neil, "Equilibrium of Totally Unneutralized Plasmas," *Physics Today* **39**, S-62 (1986).
4. C. F. Driscoll, "Containment of Single-Species Plasmas at Low Energies," in *Low Energy Antimatter* (David Cline, ed.), 184-195. Singapore: World Scientific (1986).
5. D. H. E. Dubin, T. M. O'Neil and C. F. Driscoll, "Transport Toward Thermal Equilibrium in a Pure Electron Plasma," *Proc. of Workshop of U.S.-Japan Joint Institute for Fusion Theory Program,* 265-279, Nagoya, Japan (1986).
6. T. M. O'Neil, C. F. Driscoll and D. H. E. Dubin, "Like Particle Transport: A New Theory and Experiments with Pure Electron Plasmas," *Proceedings of the International Workshop on Small Scale Turbulence and Anomalous Transport in Magnetized Plasmas* (D. Gresillon and M. A. Dubois, eds.), 293-308, Editions de Physique, Orsay (1987).
7. J. D. Crawford, S. Johnston, A. N. Kaufman and C. Oberman, "Theory of Beat-Resonant Coupling of Electrostatic Modes," *Phys. Fluids* **29**, 3219 (1986).
8. A. W. Hyatt, C. F. Driscoll and J. H. Malmberg, "Measurement of the Anisotropic Temperature Relaxation Rate in a Pure Electron Plasma," *Phys. Rev. Lett.* **59**, 2975 (1987).
9. D. H. E. Dubin and T. M. O'Neil, "Computer Simulation of Ion Clouds in a Penning Trap," *Phys. Rev. Letters* **60**, 511 (1988).
10. C. F. Driscoll, J. H. Malmberg and K. S. Fine, "Observation of Transport to Thermal Equilibrium in Pure Electron Plasmas," *Phys. Rev. Lett.* **60**, 1290 (1988).
11. D. H. E. Dubin and T. M. O'Neil, "Two-Dimensional Guiding-Center Transport of a Pure Electron Plasma," *Phys. Rev. Lett.* **60**, 1286 (1988).
12. T. M. O'Neil, "Plasmas with a Single Sign of Charge," in *Nonneutral Plasma Physics* (C. W. Roberson and C. F. Driscoll, eds.), AIP Conf. Proc. **175**, 1-25 (1988).
13. J. H. Malmberg, C. F. Driscoll, B. Beck, D. L. Eggleston, J. Fajans, K. S. Fine, X-P. Huang and A. W. Hyatt, "Experiments with Pure Electron Plasmas," in *Nonneutral Plasma Physics* (C. W. Roberson and C. F. Driscoll, eds.), AIP Conf. Proc. **175**, 28-71 (1988).
14. C. F. Driscoll, J. H. Malmberg, K. S. Fine, R. A. Smith, X.-P. Huang and R. W. Gould, "Growth and Decay of Turbulent Vortex Structures in Pure Electron Plasmas," in *Plasma Physics and Controlled Nuclear Fusion Research 1988*, Vol. 3, 507-514. Vienna: IAEA (1989).
15. C. F. Driscoll, R. A. Smith, X-P. Huang and J. H. Malmberg, "Growth and decay of vortex structures in pure electron plasmas," in *Structures in Confined Plasmas—Proc. of*

Workshop of U.S.-Japan Joint Institute for Fusion Theory Program, Report No. NIFS-PROC-2, 69-76. Nagoya: National Institute for Fusion Science (1990).

16. D. H. E. Dubin, "Correlation Energies of Simple Bounded Coulomb Lattices," *Phys. Rev. A***40**, 1140 (1989).
17. R. A. Smith, "Phase-Transition Behavior in a Negative-Temperature Guiding-Center Plasma," *Phys. Rev. Lett.* **63**, 1479 (1989).
18. C. F. Driscoll, "Observation of an Unstable $l = 1$ Diocotron Mode on a Hollow Electron Column," *Phys. Rev. Lett.* **64**, 645 (1990).
19. R. A. Smith and M. N. Rosenbluth, "Algebraic Instability of Hollow Electron Columns and Cylindrical Vortices," *Phys. Rev. Lett.* **64**, 649 (1990).
20. K. S. Fine, C. F. Driscoll and J. H. Malmberg, "Measurements of a Nonlinear Diocotron Mode in Pure Electron Plasmas," *Phys. Rev. Lett.* **63**, 2232 (1989).
21. R. A. Smith and T. M. O'Neil, "Nonaxisymmetric Thermal Equilibria of a Cylindrically Bounded Guiding Center Plasma or Discrete Vortex System," to appear in *Physics of Fluids B* (1990).
22. C. F. Driscoll and K. S. Fine, "Experiments on Vortex Dynamics in Pure Electron Plasmas," *Phys. Fluids B* **2**, 1359 (1990).
23. D. H. E. Dubin, "First-Order Anharmonic Correction for the Free Energy of a Coulomb Crystal in Periodic Boundary Conditions," *Phys. Rev. A* **42**, 4972-4982 (1990).
24. C. F. Driscoll, "Wave and Vortex Dynamics in Pure Electron Plasmas," to appear in AIP series.
25. D. H. E. Dubin and T. M. O'Neil, "Pure Ion Plasmas, Liquids and Crystals," to appear in AIP series and Edmonton Workshop proceedings.
26. D. H. E. Dubin, "Theory of Electrostatic Fluid Modes in a Cold Spheroidal Nonneutral Plasma," submitted to *Phys. Rev. Lett.*
27. K. S. Fine, C. F. Driscoll, J. H. Malmberg and T. B. Mitchell, "Measurements of Symmetric Vortex Merger in Pure Electron Plasmas," in preparation.
28. R. A. Smith, "Maximization of Vortex Entropy as an Organizing Principle in Intermittent, Decaying, Two-Dimensional Turbulence," to appear in *Phys. Rev. A.*

Theses

29. A. W. Hyatt, "Measurement of the Anisotropic Temperature Relaxation Rate in a Magnetized Pure Electron Plasma," Ph.D. Dissertation (1988).
30. K. S. Fine, "Experiments with the $l = 1$ Diocotron Mode," Ph.D. Dissertation (1988).

Invited Papers

31. C. F. Driscoll, "Pure Electron Plasma Experiments," *Proceedings of the Third International EBIS Workshop* (V. Kostroun, ed.), Cornell Univ., Ithaca, NY (1985).

32. J. H. Malmberg, "Pure Electron Plasmas," Plasma Div., APS, San Diego, CA, *APS Bull.* **30**, 1544 (1985).

33. D. H. E. Dubin, "Transport Towards Thermal Equilibrium in a Pure Electron Plasma," U.S.-Japan Workshop on Statistical Physics, Nagoya, Japan (1986).

34. T. M. O'Neil, C. F. Driscoll and D. H. E. Dubin, "Like Particle Transport: A New Theory and Experiments with Pure Electron Plasmas," in *Turbulence and Anomalous Transport in Magnetized Plasmas,* Proceedings of the International Workshop on Small Scale Turbulence and Anomalous Transport in Magnetized Plasmas, Corsica, France - 1986 (D. Gresillon and M. A. Dubois, eds.), 293-308. Editions de Physique, Orsay, (1987).

35. D. H. E. Dubin, "Computer Simulation of Ion Clouds in Traps," *Bull. Am. Phys. Soc.* **33**, 1050 (1988).

36. J. H. Malmberg, C. F. Driscoll, B. Beck, D. L. Eggleston, J. Fajans, K. Fine, X.-P. Huang and A. W. Hyatt, "Experiments with Pure Electron Plasmas," Nonneutral Plasma Physics Symposium, Washington, D.C. (1988).

37. T. M. O'Neil, "Plasmas with a Single Sign of Charge," Nonneutral Plasma Physics Symposium, Washington, D.C. (1988).

38. C. F. Driscoll, J. H. Malmberg, K. S. Fine, R. A. Smith, X-P. Huang and R. W. Gould, "Growth and Decay of Turbulent Vortex Structures in Pure Electron Plasmas," Twelfth Int. Conf. on Plasma Physics and Controlled Nuclear Fusion Research, IAEA, Nice, France (1988).

39. D. H. E. Dubin, "A Two-Dimensional Theory of Guiding Center Transport," Int. Workshop on Nonlinear Phenomena in Vlasov Plasmas, Corsica (1988).

40. D. H. E. Dubin and S. L. Gilbert, "Pure Ion Plasmas, Liquids and Crystals," *Bull. Am. Phys. Soc.* **33**, 1977 (1988).

41. C. F. Driscoll, "Experiments on Vortex Dynamics in Pure Electron Plasmas," *Bull. Am. Phys. Soc.* **34**, 2001 (1989).

42. D. H. E. Dubin and T. M. O'Neil, "Theory of Strongly-Correlated Pure Ion Plasmas in Penning Traps," in *Strongly Coupled Plasma Physics,* (S. Ichimaru, editor), Elsevier Science Pub. B.V./Yamada Science Foundation, 189-200 (1990).

43. D. H. E. Dubin, "Strongly Correlated Trapped Pure Ion Plasmas," to appear in *Proc. of 1989 International Conference on Plasma Physics*, New Delhi, India (1989).

44. T. M. O'Neil, "Plasmas with a Single Sign of Charge (A Review of Recent Theory and Experiment," Sherwood Theory Conference, Williamsburg, VA (1990).

45. C. F. Driscoll, "Wave and Vortex Dynamics in Pure Electron Plasmas," Topical Conference on Research Trends in Nonlinear and Relativistic Effects in Plasmas, La Jolla, CA (1990).

46. D. H. E. Dubin and T. M. O'Neil, "Pure Ion Plasmas, Liquids and Crystals," Topical Conference on Research Trends in Nonlinear and Relativistic Effects in Plasmas, La Jolla, CA (1990).

47. D. H. E. Dubin and T. M. O'Neil, "Pure Ion Plasmas, Liquids and Crystals," Workshop on Nonlinear and Chaotic Phenomena in Plasma Solids and Fluids, Edmonton, Canada (1990).

Contributed Papers

48. T. M. O'Neil, "Cross Magnetic Field Transport Due to Like Particle Collisions," Sherwood Theory Conference, Lake Tahoe, 1R19 (1984).
49. C. F. Driscoll, K. S. Fine and J. H. Malmberg, "Reduction of Radial Losses in a Pure Electron Plasma," Plasma Div., APS, Boston, *APS Bull.* **29**, 1279 (1984).
50. T. M. O'Neil and R. J. Menegus, "Cross Magnetic Field Transport Due to Like Particle Collisions," Plasma Div., APS, Boston, *APS Bull.* **29**, 1279 (1984).
51. A. W. Hyatt, J. H. Malmberg, C. F. Driscoll, K. Fine, B. Beck and D. Eggleston, "Observation of Anisotropic Temperature Relaxation," Plasma Div., APS, San Diego, *APS Bull.* **30**, 1552 (1985).
52. C. F. Driscoll, K. S. Fine and J. H. Malmberg, "Transport to Thermal Equilibrium in Pure Electron Plasmas," Plasma Div., APS, San Diego, *APS Bull.* **30**, 1552 (1985).
53. T. M. O'Neil and D. H. E. Dubin, "A New Theory of Transport Due to Like Particle Collisions," Plasma Div., APS, San Diego, *APS Bull.* **30**, 1552 (1985).
54. A. W. Hyatt, C. F. Driscoll and J. H. Malmberg, "Observation of Anisotropic Temperature Relaxation," Plasma Div., APS, Baltimore, *APS Bull.* **31**, 1391 (1986).
55. K. S. Fine, W. D. White, J. H. Malmberg and C. F. Driscoll, "Induced Damping of a Diocotron Wave and Associated Transport," Plasma Div., APS, Baltimore, *APS Bull.* **31**, 1391 (1986).
56. C. F. Driscoll, K. S. Fine and J. H. Malmberg, "Enhanced Like-Particle Transport in Pure Electron Plasmas," Plasma Div., APS, Baltimore, *APS Bull.* **31**, 1392 (1986).
57. D. H. E. Dubin and T. M. O'Neil, "A New Theory of Transport Due to Like Particle Collisions," Plasma Div., APS, Baltimore, *APS Bull.* **31**, 1392 (1986).
58. C. F. Driscoll, J. H. Malmberg and K. S. Fine, "Like-Particle Transport Scaling as B^{-1} in Pure Electron Plasmas," Plasma Div., APS, San Diego, *APS Bull.* **32**, 1754 (1987).
59. T. M. O'Neil and D. H. E. Dubin, "$\mathbf{E}\times\mathbf{B}$ Transport in a Magnetically Confined Nonneutral Plasma," Plasma Div., APS, San Diego, *APS Bull.* **32**, 1754 (1987).
60. A. W. Hyatt, C. F. Driscoll and J. H. Malmberg, "Measurement of the Anisotropic Temperature Relaxation Rate in a Pure Electron Plasma," Plasma Div., APS, San Diego, *APS Bull.* **32**, 1755 (1987).
61. K. S. Fine, C. F. Driscoll and J. H. Malmberg, "Large Amplitude and Finite Length Effects in Diocotron Modes," Plasma Div., APS, San Diego, *APS Bull.* **32**, 1755 (1987).
62. R. A. Smith, M. N. Rosenbluth, C. F. Driscoll and T. M. O'Neil, "Two-Dimensional Shear-Flow Instabilities in a Pure Electron Plasma," Plasma Div., APS, Hollywood, *APS Bull.* **33**, 1898 (1988).

63. C. F. Driscoll, J. H. Malmberg and R. A. Smith, "Diocotron Instability Rates and Eigenfunctions for Hollow Electron Columns," Plasma Div., APS, Hollywood, *APS Bull.* **33**, 1898 (1988).

64. X.-P. Huang, C. F. Driscoll and J. H. Malmberg, "Dynamical and Statistical Measurements on Plasmas Exhibiting Vortex Growth and Decay," Plasma Div., APS, Hollywood, *APS Bull.* **33**, 1898 (1988).

65. K. S. Fine, C. F. Driscoll and J. H. Malmberg, "Measurements of a Nonlinear Diocotron Mode," Plasma Div., APS, Hollywood, *APS Bull.* **33**, 1899 (1988).

66. D. H. E. Dubin, "Correlation Properties of Simple Bounded Coulomb Lattices," *APS Bull.* **33**, 1899 (1988).

67. K. S. Fine, C. F. Driscoll, T. B. Mitchell and J. H. Malmberg, "Dynamics and Instabilities of 2D Electron Plasma Vortices," Plasma Div., APS, Anaheim, *APS Bull.* **34**, 1932 (1989).

68. C. F. Driscoll, "Observation of an $l = 1$ Diocotron Instability on Hollow Electron Columns," Plasma Div., APS, Anaheim, *APS Bull.* **34**, 1932 (1989).

69. R. A. Smith and T. M. O'Neil, "Nonaxisymmetric Thermal Equilibria of a Non-neutral Guiding Center Plasma in a Cylindrical Trap," Plasma Div., APS, Anaheim, *APS Bull.* **34**, 1934 (1989).

70. D. H. E. Dubin, "Structure of a Bounded Coulomb Lattice," Plasma Div., APS, Anaheim, *APS Bull.* **34**, 1934 (1989).

71. K. S. Fine, C. F. Driscoll, T. B. Mitchell and J. H. Malmberg, "Dynamics and Instabilities of 2D Electron Plasma Vortices," Fluid Dynamics Div., APS, Palo Alto, *APS Bull.* **34**, 2308 (1989).

72. R. A. Smith and M. N. Rosenbluth, "Algebraic Instability of Cylindrical Shear Flows," Fluid Dynamics Div., APS, Palo Alto, *APS Bull.* **34**, 2336 (1989).

73. C. F. Driscoll, "Observation of an $l = 1$ Shear Instability on Hollow Electron Columns," Fluid Dynamics Div., APS, Palo Alto, *APS Bull.* **34**, 2336 (1989).

74. R. A. Smith and T. M. O'Neil, "Maximum Entropy Equilibria of a Nonneutral Guiding-Center Plasma," Sherwood Theory Conference, Williamsburg, VA (1990).

75. R. A. Smith, "Phase Transition Behavior in a Negative Temperature Guiding Center Plasma or Vortex Gas," Fourth Univ. of California Conf. on Statistical Mechanics, Santa Barbara (1990).

76. R. A. Smith and T. M. O'Neil, "Thermal Equilibria of a Nonneutral Guiding Center Plasma in a Cylindrical Trap," *Bull. Am. Phys. Soc.* **35**, 2134 (1990).

77. K. S. Fine, C. F. Driscoll, T. B. Mitchell and J. H. Malmberg, "Symmetric Vortex Merger in Pure Electron Plasmas," *Bull. Am. Phys. Soc.* **35**, 2135 (1990).

78. T. B. Mitchell, C. F. Driscoll and K. S. Fine, "Observation of a Wall-Induced Instability of Two Interacting Vortices," *Bull. Am. Phys. Soc.* **35**, 2135 (1990).

79. X.-P. Huang, C. F. Driscoll and J. H. Malmberg, "Measurements of the Decay of Two-Dimensional Turbulence in Pure Electron Plasmas," *Bull. Am. Phys. Soc.* **35**, 2135 (1990).

80. D. H. E. Dubin, "Theory of Electrostatic Normal Modes in a Cold Spheroidal Nonneutral Plasma," *Bull. Am. Phys. Soc.* **35**, 2135 (1990).

81. R. A. Smith and T. M. O'Neil, "Statistics of Point Vortices in a Circular Boundary," *Bull. Am. Phys. Soc.* **35**, 2227 (1990).

82. K. S. Fine, C. F. Driscoll, T. B. Mitchell and J. H. Malmberg, "Experiments on Symmetric Vortex Merger," *Bull. Am. Phys. Soc.* **35**, 2267 (1990).

83. C. F. Driscoll, "Observation of an Unexpected $l = 1$ Instability on a Cylindrical Shear Flow," *Bull. Am. Phys. Soc.* **35**, 2247 (1990).